UNIVERSIDADE FEDERAL DO PARANÁ

DIEGO ANDRÉS CASAS TORO

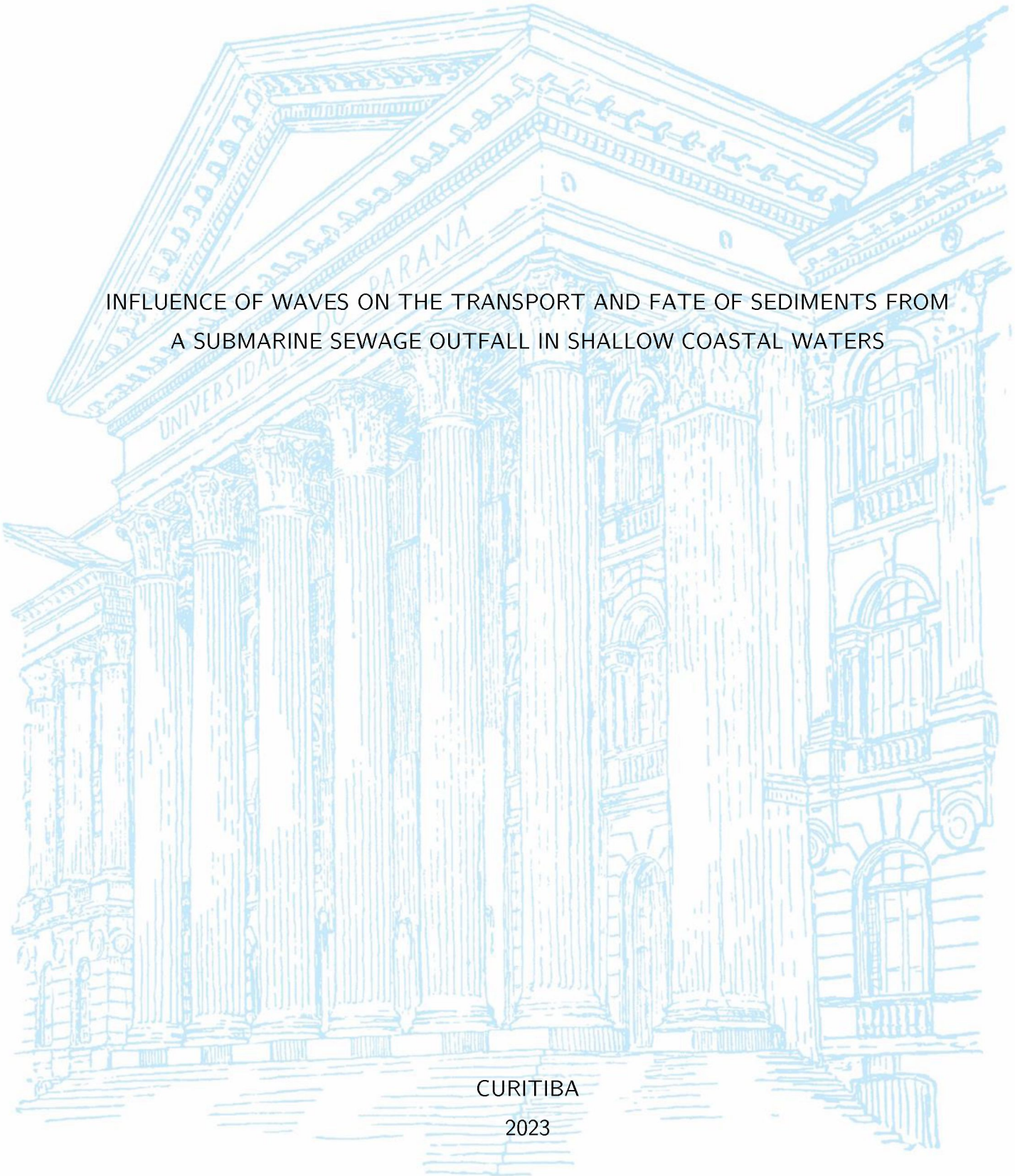

INFLUENCE OF WAVES ON THE TRANSPORT AND FATE OF SEDIMENTS FROM A SUBMARINE SEWAGE OUTFALL IN SHALLOW COASTAL WATERS

CURITIBA

2023

DIEGO ANDRÉS CASAS TORO

INFLUENCE OF WAVES ON THE TRANSPORT AND FATE OF SEDIMENTS FROM A SUBMARINE SEWAGE OUTFALL IN SHALLOW COASTAL WATERS

Dissertação apresentada ao Programa de Pós-Graduação em Engenharia de Recursos Hídricos e Ambiental, Setor de Tecnologia, Universidade Federal do Paraná, como requisito parcial à obtenção do título de Mestre em Engenharia de Recursos Hídricos e Ambiental.

Orientador: Prof. Dr. Tobias Bleninger

Coorientador: Prof. Dr. Maurício Gobbi

Coorientadora: Dr.ª Silene Baptistelli

CURITIBA

2023

DADOS INTERNACIONAIS DE CATALOGAÇÃO NA PUBLICAÇÃO (CIP)
UNIVERSIDADE FEDERAL DO PARANÁ
SISTEMA DE BIBLIOTECAS – BIBLIOTECA DE CIÊNCIA E TECNOLOGIA

Toro, Diego Andrés Casas
Influence of waves on the transport and fate of sediments from a submarine sewage outfall in shallow coastal waters / Diego Andrés Casas Toro. – Curitiba, 2023.
1 recurso on-line : PDF.

Dissertação (Mestrado) - Universidade Federal do Paraná, Setor de Tecnologia, Programa de Pós-Graduação em Engenharia de Recursos Hídricos e Ambiental.

Orientador: Tobias Bernward Bleninger
Coorientadores: Maurício Felga Gobbi; Silene Cristina Baptistelli

1. Emissários submarinos. 2. Ondas oceânicas. 3. Sedimentos em suspensão. I. Universidade Federal do Paraná. II. Programa de Pós-Graduação em Engenharia de Recursos Hídricos e Ambiental. III. Bleninger, Tobias Bernward. IV. Gobbi, Maurício Felga. V. Baptistelli, Silene Cristina. VI. Título.

Bibliotecário: Elias Barbosa da Silva CRB-9/1894

TERMO DE APROVAÇÃO

Os membros da Banca Examinadora designada pelo Colegiado do Programa de Pós-Graduação ENGENHARIA DE RECURSOS HÍDRICOS E AMBIENTAL da Universidade Federal do Paraná foram convocados para realizar a arguição da Dissertação de Mestrado de **DIEGO ANDRES CASAS TORO** intitulada: **Influence of waves on the transport and fate of sediments from a submarine sewage outfall in shallow coastal waters**, sob orientação do Prof. Dr. TOBIAS BERNWARD BLENINGER, que após terem inquirido o aluno e realizada a avaliação do trabalho, são de parecer pela sua APROVAÇÃO no rito de defesa.

A outorga do título de mestre está sujeita à homologação pelo colegiado, ao atendimento de todas as indicações e correções solicitadas pela banca e ao pleno atendimento das demandas regimentais do Programa de Pós-Graduação.

CURITIBA, 03 de Fevereiro de 2023.

Assinatura Eletrônica
03/02/2023 16:48:03.0
TOBIAS BERNWARD BLENINGER
Presidente da Banca Examinadora

Assinatura Eletrônica
06/02/2023 09:12:30.0
JOSÉ EDUARDO GONÇALVES
Avaliador Interno (INSTITUTO TECNOLOGICO SIMEPAR)

Assinatura Eletrônica
06/02/2023 16:03:05.0
EDUARDO PUHL
Avaliador Externo (UNIVERSIDADE FEDERAL DO RIO GRANDE DO SUL)

Assinatura Eletrônica
06/02/2023 09:03:57.0
ALEXANDRE KOLODYNSKIE GUETTER
Avaliador Interno (UNIVERSIDADE FEDERAL DO PARANÁ)

Assinatura Eletrônica
03/02/2023 16:51:39.0
MAURÍCIO FELGA GOBBI
Coorientador(a)

Assinatura Eletrônica
06/02/2023 11:37:44.0
SILENE CRISTINA BAPTISTELLI
Coorientador(a)

RESUMO

O presente trabalho visa estudar os efeitos das ondas sobre o transporte e destino de sedimentos oriundos de emissários submarinos de esgotos em águas relativamente rasas. Um modelo hidrodinâmico com e sem efeitos de ondas foi implementado, calibrado e validado para um estudo de caso na Baixada Santista, estado de São Paulo, Brasil. Foram incluídas em ambos os casos descargas de sedimento suspenso de cinco emissários. Para estudar a influência das condições de ondas, foram definidos três períodos correspondentes a ondas leves, médias e fortes. Os resultados dos modelos de apenas correntes e onda-corrente foram comparados para identificar diferenças no transporte e destino do sedimento dos emissários devido à ação das ondas. Verificou-se que, se as ondas não forem consideradas, o modelo simula um processo de deposição contínua que resulta em acúmulo irrealista de sedimentos no leito. Foi observada ressuspensão significativa induzida por ondas nas proximidades dos difusores dos emissários, mesmo durante condições de ondas leves. Sob condições de ondas médias e fortes, o sedimento afetado pode ser transportado por correntes litorâneas e se assentar longe do local da descarga, chegando às costas e canais próximos. Os eventos de ressuspensão observados são controlados por movimentos orbitais de onda próximos ao leito, que agitam os sedimentos. Em geral, os resultados indicam que os modelos acoplados de onda-corrente podem ajudar a entender melhor o destino dos poluentes associados aos sedimentos oriundos de emissários e a identificar áreas de preocupação ambiental a longo prazo. Em conclusão, sugere-se que futuros estudos considerem os efeitos potenciais das ondas superficiais sobre o projeto e as condições operacionais de emissários submarinos de esgotos, especialmente para emissários que descarregam em águas relativamente rasas.

Palavras-chave: Emissário submarino. Interação onda-corrente. Ressuspensão de sedimento.

ABSTRACT

The present work aims to study the effects of waves on the transport and fate of sediments from submarine wastewater outfalls in relatively shallow waters. A hydrodynamic model both with and without wave effects was implemented, calibrated and validated for a case study in Baixada Santista, São Paulo state, Brazil. Suspended sediment discharges from five outfalls were included in both cases. To study the influence of wave conditions, three periods corresponding to mild, mean and strong waves were defined. The results from current-only and wave-current models were compared to identify differences in the transport and fate of outfall effluent sediments due to wave action. It was found that, if waves are not considered, the model simulates a continuous deposition process that results in unrealistic bed sediment accumulation. Significant wave-induced resuspension was observed in the vicinity of the outfall diffusers, even during mild wave conditions. Under mean and strong wave conditions, the affected sediment can be transported further by longshore currents and settle far away from the discharge location, reaching nearby coasts and channels. The observed events of resuspension are controlled by near-bed wave orbital motions that stir up bed sediments. Overall, results indicate that coupled wave-current models can help to better understand the fate of sediment-attached pollutants from outfalls and to identify areas of long-term environmental concern. In conclusion, it is suggested that future studies consider the potential effects of surface waves on the design and operational conditions of submarine sewage outfalls, especially for outfalls that discharge in relatively shallow waters.

Keywords: Marine outfall. Wave-current interaction. Sediment resuspension.

RESUMEN

El presente trabajo tiene como objetivo estudiar los efectos del oleaje en el transporte y destino de sedimentos procedentes de emisarios submarinos de aguas residuales en aguas relativamente poco profundas. Se implementó, calibró y validó un modelo hidrodinámico con y sin efectos de oleaje para un estudio de caso en Baixada Santista, estado de São Paulo, Brasil. En ambos casos se incluyeron descargas de sedimento en suspensión procedentes de cinco emisarios. Para estudiar la influencia de las condiciones de oleaje, se definieron tres períodos correspondientes a oleaje leve, medio y fuerte. Se compararon los resultados de los modelos de solo corriente y de oleaje-corriente para identificar las diferencias en el transporte y el destino de los sedimentos de los emisarios debido a la acción de las olas. Se comprobó que, si no se tiene en cuenta el oleaje, el modelo simula un proceso de deposición continua que da lugar a una acumulación de sedimentos poco realista en el lecho. Se observó resuspensión significativa inducida por el oleaje en las proximidades de los difusores de los emisarios, incluso en condiciones de oleaje leve. En condiciones de oleaje medio y fuerte, el sedimento afectado puede ser transportado por corrientes litorales y asentarse lejos del lugar de descarga, alcanzando costas y canales cercanos. Los fenómenos de resuspensión observados son controlados por movimientos orbitales del oleaje cerca del lecho que agitan los sedimentos. En general, los resultados indican que los modelos acoplados de oleaje y corrientes pueden ayudar a comprender mejor el destino de los contaminantes adheridos a los sedimentos procedentes de emisarios y a identificar zonas de preocupación medioambiental a largo plazo. En conclusión, se sugiere que en futuros estudios se tengan en cuenta los efectos potenciales del oleaje sobre el diseño y las condiciones operativas de emisarios submarinos de aguas residuales, especialmente en el caso de emisarios que descargan en aguas relativamente poco profundas.

Palabras clave: Emisario submarino. Interacción onda-corriente. Resuspensión de sedimento.

CONTENTS

Influence of waves on the transport and fate of sediments from a submarine sewage outfall in shallow coastal waters

Diego A. Casas*† Tobias Bleninger† Maurício F. Gobbi‡ Silene C. Baptistelli§

Abstract

The present work aims to study the effects of waves on the transport and fate of sediments from submarine wastewater outfalls in relatively shallow waters. A hydrodynamic model both with and without wave effects was implemented, calibrated and validated for a case study in Baixada Santista, São Paulo state, Brazil. Suspended sediment discharges from five outfalls were included in both cases. To study the influence of wave conditions, three periods corresponding to mild, mean and strong waves were defined. The results from current-only and wave-current models were compared to identify differences in the transport and fate of outfall effluent sediments due to wave action. It was found that, if waves are not considered, the model simulates a continuous deposition process that results in unrealistic bed sediment accumulation. Significant wave-induced resuspension was observed in the vicinity of the outfall diffusers, even during mild wave conditions. Under mean and strong wave conditions, the affected sediment can be transported further by longshore currents and settle far away from the discharge location, reaching nearby coasts and channels. The observed events of resuspension are controlled by near-bed wave orbital motions that stir up bed sediments. Overall, results indicate that coupled wave-current models can help to better understand the fate of sediment-attached pollutants from outfalls and to identify areas of long-term environmental concern. In conclusion, it is suggested that future studies consider the potential effects of surface waves on the design and operational conditions of submarine sewage outfalls, especially for outfalls that discharge in relatively shallow waters.

1 Introduction

Coastal wastewater disposal is often done by means of submarine outfalls. These are pipelines designed to discharge raw or partially treated wastewater to the seabed at a certain distance from the coast. At the discharge location, the outfall has a diffuser that facilitates the dilution of the effluent in seawater. The dilution process depends on several factors: wastewater flowrate, water depth, diffuser geometry and oceanic conditions such as currents, stratification, tides and turbulence (Tate et al. 2016). The analysis and modeling of outfall plumes is generally performed considering three regions: near field; mid field; and far field. In the near field, plume dynamics is dominated by the outflow; in the far field, plume behavior is dominated by ocean currents; and the mid field is a transition zone (Morelissen et al. 2013). Most of the dilution occurs in the near field, while in the far field, the plume is mainly transported by ambient currents with a much lower mixing dominated by natural processes (Roberts 1991). Because of this, studies on long-term transport and fate of outfall plume constituents are ultimately conducted in the far-field zone.

*Corresponding author: diego.casas@ufpr.br
†Graduate Program of Water Resources and Environmental Engineering, Federal University of Paraná, Curitiba, Brazil
‡Graduate Program of Environmental Engineering, Federal University of Paraná, Curitiba, Brazil
§Sanitation Company of São Paulo State, São Paulo, Brazil

Far-field plume modeling can be performed using a Lagrangian approach (e.g., Veríssimo and Martins 2016; Roberts and Villegas 2017). However, for long periods and large complex domains, particle-tracking models may become inaccurate and time consuming, so Eulerian models that solve the advection-diffusion equation may be more appropriate (Zhao et al. 2011). Hydrodynamic and ocean circulation models such as Delft3D, MIKE 21/3, MOHID and ROMS, coupled with advection-diffusion or particle-tracking modules, are generally used for outfall plume modeling. These models force Eulerian or Lagrangian tracer equations with hydrodynamics fields resulting from solving the Reynolds-averaged Navier-Stokes equations in three dimensional or depth-averaged form under Boussinesq and hydrostatic assumptions. The use of non-hydrostatic models have been recently studied for cross-flow scenarios (Ho et al. 2021).

To correctly simulate wastewater plume dispersion in coastal and estuarine environments, an accurate representation of currents is required. Ocean currents are induced by a variety of physical processes such as tides, wind and density gradients, so, far-field outfall modeling depends on the inclusion of those processes as forcings. For outfalls in coastal regions, the most elemental models may be depth-averaged and forced only by tides, usually prescribed as tidal constituents, in the absence of water level measurements at domain boundaries (Tomicic et al. 2001). However, in the case of estuarine systems, not only the tides but also the fluvial discharges are important forcings to consider in the far-field modeling (e.g., Neves 2006). In some regions, wind can have a strong effect on currents, so a representative wind field must be specified as forcing. Roberts and Villegas (2017) highlighted the importance of wind measurements made directly over the water for a far-field model of an outfall in a large estuary.

Spatial variability in water temperature and salinity is associated with water column stratification and density gradients that induce currents. For a more detailed simulation of far-field conditions, temperature and salinity can be coupled with hydrodynamics to account for their effects on both currents and water quality (see, e.g., Pritchard et al. 2013; Falkenberg et al. 2016; Birocchi et al. 2021). Furthermore, it is possible to implement very sophisticated three-dimensional far-field models that not only consider all of the above forcings and processes but also sea surface fluxes such as heat (Veríssimo and Martins 2016) and freshwater (precipitation and evaporation) (Uchiyama et al. 2014; Ostoich et al. 2018; Mrša Haber et al. 2020). Under current common practice, a two-dimensional depth-averaged simulation is acceptable when the receiving body of water is relatively shallow ($\leq$15–20 m) and vertically well-mixed (Pritchard et al. 2013; Tate et al. 2016; Roberts and Villegas 2017).

Apart from the effects on water quality, wastewater disposal in coastal waters is known to produce sediment pollution. Sediment pollution can occur when contaminated particles are directly released into a body of water or when suspended or bed sediments absorb water contaminants (Megahan 1999). The seabed in coastal areas receiving wastewater discharges is commonly characterized by a superficial layer of organic mud with black or gray coloration (Wasserman et al. 2000; Gkaragkouni et al. 2021). The effects of sewage discharges on bed sediment bacterial concentrations and benthic life have been reported as early as the mid-20th century (Nusbaum and Garver 1955; Rittenberg et al. 1958; Watkins 1961). Elevated concentrations of different types of pollutants have been reported in sediment samples in the vicinity of marine outfalls, e.g., heavy metals (Hershelman et al. 1981; Soto-Jiménez et al. 2001; Gkaragkouni et al. 2021), toxic organic contaminants (Moon et al. 2008; Akdemir and Dalgic 2021) and contaminants of emerging concern such as microplastics (Reed et al. 2018) and pharmaceutical products (Maruya et al. 2012).

Near-field particle deposition from outfalls jets in stagnant and flowing environments have been extensively investigated (Neves and Fernando 1995; Bleninger and Carmer 2000; Lane-Serff and Moran 2005; Cuthbertson et al. 2008; Terfous et al. 2016). However, transport and fate of outfall sediments in the far field have not received as much attention although it is phenomenologically understood (e.g.,

Herring 1980). For example, Bodeen et al. (1989) developed a software that employs progressive vector diagrams to estimate the deposition of outfall particulates from current velocity measurements. Hodgins et al. (2000) implemented a three-dimensional particle deposition model for sewage solids from a large submarine outfall under tidal currents. Ferré et al. (2010) applied a one-dimensional vertical model to a number of current measurement sites in order to study sediment transport in a continental shelf affected by sewage outfalls. More recently, Tate et al. (2019) estimated particle settlement and resuspension using a combination of simplified formulas, current measurements and outputs of a near-field Lagrangian plume model.

By analyzing the previously referenced studies, it is noticed that there is a gap between the current practice of far-field outfall modeling and studies on the fate and transport of solid particles from outfall effluents. Generally, modeling efforts focus on studying wastewater plume concentration development in the near and far fields with little or no detail on the solid fraction of the plume. On the other hand, studies aimed to understand the fate of effluent solid particles usually rely on simplified estimates of particle movement (e.g., Herring 1980; Tate et al. 2019). Detailed studies on effluent sediments are important because once the sewage plume is discharged into seawater, solid particles move and interact with other constituents under complex ambient forces. Eventually, since most of the solid mass in the effluent is denser than water, particles start to settle under gravity as they are advected by mean currents. After deposition, sediments are susceptible to be disturbed by other agents. Coastal processes such as internal or surface waves can resuspend solid particles, which then undergo further transport by currents along the shelf (Lee et al. 2003). In particular, in shallow waters, the combined action of surface waves and currents may generate frequent events of resuspension that can release dissolved metals and nutrients (Kalnejais et al. 2010). Also, sediment resuspension can act as a bacterial input mechanism for the overlying water column (Gao et al. 2013).

Although the influence of internal waves on outfall sediment resuspension has been studied before (Tate et al. 2019), surface waves have only been pointed out as a potentially relevant process with no detailed studies on the matter. During field studies in the vicinity of an outfall, Wu et al. (1991) observed current-induced sediment resuspension; however, the authors mentioned that surface waves may also be contributors. Lee et al. (2003) analyzed a large array of field measurements of a continental shelf influenced by a submarine outfall and mentioned surface waves as a dominant process for sediment resuspension in some parts of the shelf. In a study in estuarine waters, Neves (2006) suggested a relationship between measurements of wave orbital motion and events of sediment resuspension near an outfall diffuser. After developing a coupling algorithm for near and far-field modeling of outfalls, Bleninger (2006) proposed future work on the inclusion of polluted solid particles and their interaction with waves.

To the knowledge of the authors, no detailed research has been done on assessing the relative importance of surface waves in far-field modeling of submarine outfalls. Actually, including waves in far-field outfall models is not common in the current practice, even though they might have significant effects at smaller spatial scales (Zhao et al. 2011). Only a few academic studies have included waves into the hydrodynamic modeling of outfalls (e.g., Inan 2019; Kim et al. 2021); however, they are neither concerned with assessing the effects of waves nor do they include sediment transport. Given the lack of studies on the relevance of waves in far-field outfall models, their inclusion in academic or engineering studies is almost discretionary. In this regard, the present study aims to make an initial attempt to assess the relative importance of waves and wave-current interactions for far-field modeling of submarine outfalls.

Considering that waves may have significant effects on outfall sediment transport, an ensemble of five submarine outfalls in the metropolitan area of Baixada Santista in São Paulo State, Brazil, was selected as a case study. There is one outfall in the Santos municipality, another in Guarujá and three in

Praia Grande (PG1, PG2 and PG3). These outfalls discharge sewage at shallow depths (<15 m), where surface waves may play a significant role in the resuspension of effluent sediment. In Baixada Santista, bed sediment quality is of concern. A recent report by the Environmental Agency of São Paulo State (CETESB 2022), showed elevated concentrations of total organic carbon, Kjeldahl nitrogen, phosphorus and *Clostridium perfringens* bacteria in sediments from the influence area of the PG1 outfall, as well as elevated concentrations of thermotolerant coliforms and *C. perfringens* in sediments near the discharge locations of the Santos and Guarujá outfalls, respectively. Several authors have found high toxicity to benthic amphipods in sediment samples in the vicinity of the Santos outfall diffuser (Abessa et al. 2005; Cesar et al. 2006; Abessa et al. 2008; Sousa et al. 2014; Vacchi et al. 2019). In particular, Vacchi et al. (2019) demonstrated that the toxicity is related to organic contaminants absorbed by the sediment particles. Furthermore, recent studies have found high levels of contaminants of emerging concern in sediments in the vicinity of the outfalls discharge locations. For example, endocrine disrupting chemicals for outfalls of Santos, Guarujá, PG1 and PG2 (Santos et al. 2018), and rhodium for Santos (Berbel et al. 2021).

Direct measurements of outfall sediment transport could provide a better understanding of the influence of the outfalls on sediment quality. Dilution and dispersion of the outfall wastewater plume can be studied by injecting a dye tracer into the effluents, as it has been done for other Brazilian outfalls (e.g., Carvalho et al. 2002). However, studying the solid fraction of the effluents requires a different approach such as adding artificial particles or tagging the existing sediment, and there is no record of such a study for the outfalls in Baixada Santista. In the absence of direct field measurements, a numerical model can provide major insights on outfall sediment transport. Consequently, the present study is concerned with the transport and fate of sediment from the five submarine outfalls in Baixada Santista under a modeling perspective. Since the outfalls discharge their effluents in relatively shallow waters exposed to the open ocean, the use of a coupled wave-current hydrodynamic model is proposed. The objective of the study is to assess the relative importance of waves and the combined action of waves an currents for far-field modeling of submarine outfall sediments. Hydrodynamic and wave propagation models for the coastal area of Baixada Santista were implemented using the Delft3D modeling suite (Deltares 2020a, 2020b). These models were calibrated and validated using field data such as water level and wave buoy measurements. Sediment transport was implemented only for the outfall effluents, so other sources of sediment were not included, e.g., streams, longshore drift, surface runoff. In order to assess the effects of wave-current interaction on sediment transport and fate, the results of standalone hydrodynamic models were compared with coupled wave-current models for mild, mean and strong wave regimes. The focus was on sediment resuspension events, and special attention was given to wave conditions that produced or enhanced the phenomenon.

2 Materials and methods

2.1 Site description

Baixada Santista is a metropolitan area located in the coastal region of São Paulo State, Brazil. It comprises nine municipalities and is served by five submarine wastewater outfalls operated by the Sanitation Company of São Paulo State (Sabesp). There is one outfall in the Santos municipality, another in Guarujá and three in Praia Grande (see Figure 1b). The Santos outfall consists of a concrete-covered steel pipe that discharges wastewater from the Santos and São Vicente municipalities into the Santos Bay. Outfalls of Guarujá and Praia Grande discharge directly to the Atlantic Ocean through high-density polyethylene

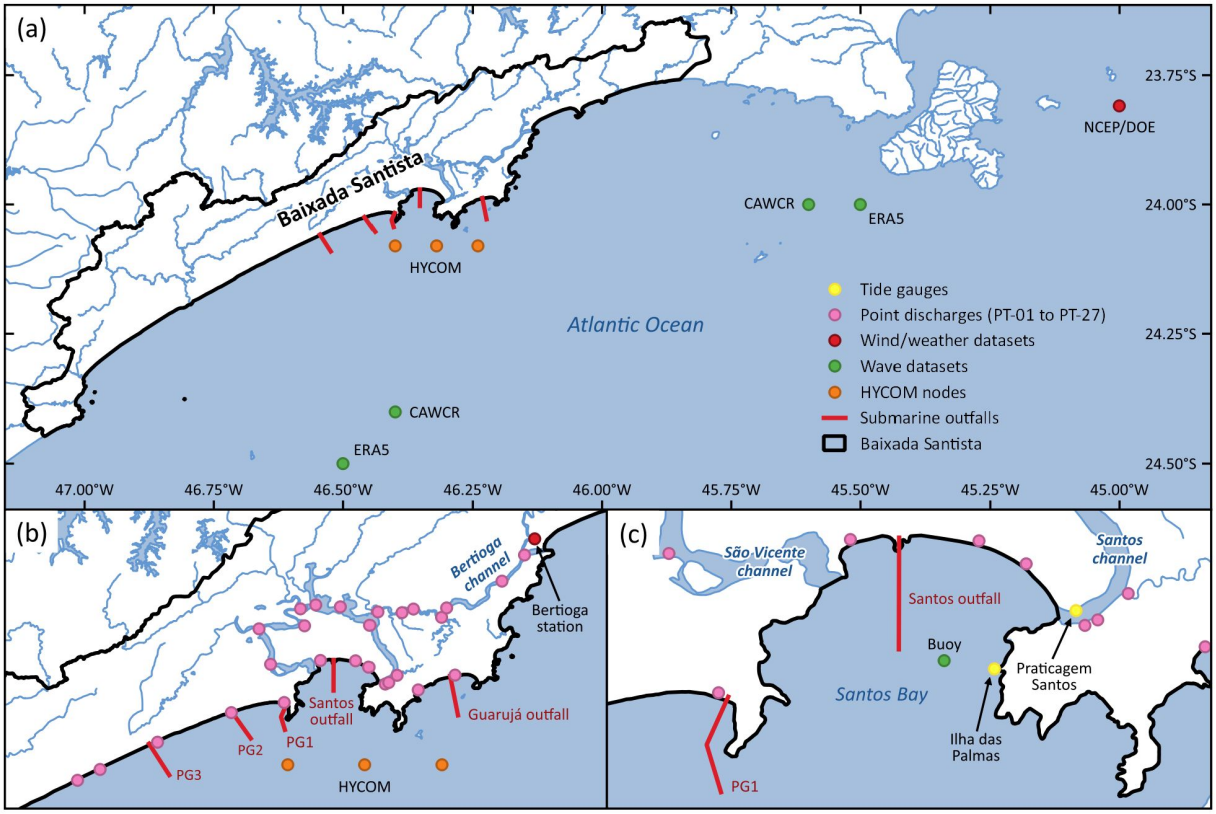

Figure 1: Location of the study area and points of interest.

Outfall	Length (m)	Diameter (m)	Depth (m)	Maximum discharge (m^3/s)
Santos	4425	1.75	11.5	5.30
Guarujá	4500	0.90	14.0	1.45
PG1	3300	1.00	14.0	1.20
PG2	3300	1.00	14.0	1.20
PG3	4095	1.00	13.0	1.40

Table 1: Characteristics of the submarine outfalls in Baixada Santista (data for 2019).

pipes. Until 2019, the effluent of Santos outfall had primary treatment with 1.5-mm screening and disinfection. Up to that year, the effluent of outfalls Guarujá and PG3 also received primary treatment, while effluents of outfalls PG1 and PG2 only received preliminary treatment. As of 2020, several engineering efforts and operational reforms have been done (e.g., primary treatment for all outfalls and outfall length extensions for PG1 and PG2). General characteristics for 2019 of the five outfalls are summarized in Table 1. It is worth noting that for the studied time periods, outfalls discharges did not reach the maximum design values.

Baixada Santista is located on a coastal plain delimited by the Serra do Mar mountain system and the Atlantic Ocean. One of the most prominent morphological features along its shoreline is the Santos estuarine system, which comprises the Santos Bay and the estuarine channels of São Vicente, Bertioga and Santos (Figure 1b,c). Santos Bay is a semi-sheltered and shallow bay (depths between 5 and 15 m). The study area presents a mainly semidiurnal tide with diurnal inequalities (Schettini et al. 2019). Inside the bay, spring and neap tides have amplitudes of about 0.6 m and 0.14 m, respectively (Harari et al. 2008). Also, the region is under the influence of cold fronts that, each, generate strong winds for about 2 days on a nearly weekly basis (Stech and Lorenzzetti 1992).

Tides are of great importance for eddy diffusivity and vertical mixing inside Santos Bay. Salinity measurements during neap and spring tides show that the estuary is weakly stratified near its head and at the entrance of the channels (Harari et al. 2008). Other studies have found that Santos Bay and its outer coastal area are well mixed during spring tides (Belém et al. 2007). Furthermore, suspended solids concentrations are of the order of $10^{-2}\,\mathrm{kg/m^3}$ and can be considered horizontally and vertically homogeneous in most of the bay, showing no significant influence of spring and neap tides (Berzin 1992).

Most of the year, the dominant wave direction is from south, with heights 1–3 m and periods of 10–12 s, and the highest waves usually come from the southwest, reaching up to 6.3 m (Pianca et al. 2010). As it is typical in the southern and southeastern Brazilian coast, the region is characterized by multi-modal sea states consisting of a locally generated wind wave system and two or more swells propagating from distant fetches (Violante-Carvalho et al. 2001; Innocentini et al. 2014). The most energetic waves in the region are associated with cold fronts and have a significant impact on the local morphodynamics (Stein and Siegle 2019).

2.2 Available data

Topographic and bathymetric data of Baixada Santista were obtained from different sources such as bathymetric surveys performed by the Santos Pilotage Service (Praticagem do Porto de Santos); nautical charts from the Brazilian Navy's Directorate of Hydrography and Navigation (DHN); the General Bathymetric Chart of the Oceans (GEBCO); the SRTM15+V2.0 global elevation grid (Tozer et al. 2019); and sparse survey data provided by Sabesp.

Water level time series from tide gauges of Praticagem Santos and Ilha das Palmas were provided by DHN. Both tide gauges are located inside the Santos estuary. The former is at the entrance of the Santos channel; the latter is on an island to the east of Santos Bay. Marine climate data such as water temperature, salinity, and currents, were retrieved from nodes of the Hybrid Coordinate Ocean Model (HYCOM; Bleck 2002). Observational data of wind velocity and direction were available at the Bertioga station owned by the Brazilian National Institute of Meteorology (INMET). However, auxiliary wind fields were retrieved from an atmospheric reanalysis of the United States National Centers for Environmental Prediction (NCEP) (NCEP/DOE Reanalysis 2; Kanamitsu et al. 2002). Other required meteorological variables such as relative humidity, air temperature and net solar radiation were also extracted from the NCEP/DOE Reanalysis. Figure 1 shows the location of the tide gauges, the meteorological station and the HYCOM and NCEP/DOE global grid nodes employed in the study.

From an analysis of the drainage system of Baixada Santista, there were identified a total of 27 freshwater point discharges (PT-01 to PT-27) into the coastal area influenced by the five submarine outfalls (see Figure 1b,c). The point discharges correspond to streams and effluents with mean annual flows between 0.15 and 25.26 $\mathrm{m^3/s}$. Data on outfall discharges and sparse measurements of total suspended solids of the five submarine outfalls for 2019 were provided by Sabesp. Outfall discharge time series were analyzed for inconsistencies on a monthly frequency, replacing suspicious records with compatible records from the previous year or the following year.

Regarding the wave climate, time series of significant wave height and peak period at a buoy in Santos Bay (see Figure 1c) were provided by Fundação Centro Tecnológico de Hidráulica (FCTH). Hourly-averaged wave parameters in deep water were obtained from the European Centre for Medium Range Weather Forecasts (ECMWF) fifth generation reanalysis (ERA5; Hersbach et al. 2020) and the Collaboration for Australian Weather and Climate Research (CAWCR) wave hindcast (Smith et al. 2021). The ERA5 and CAWCR grid nodes employed for the study are shown in Figure 1a. Since wind fields are an

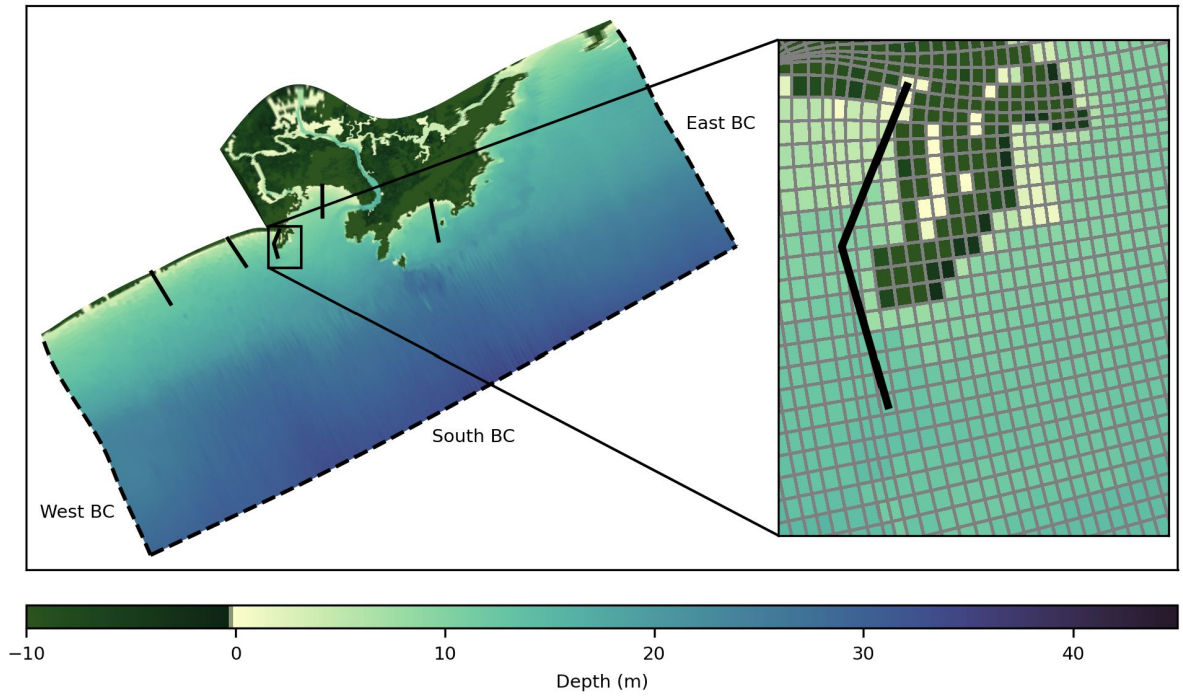

Figure 2: Delft3D-FLOW domain with interpolated bathymetry.

important input for wave propagation models, three global wind datasets were considered. In addition to ERA5 which also provides wind data, we used wind fields from the United States National Aeronautics and Space Administration (NASA) Modern-Era Retrospective Analysis for Research and Applications, version 2 (MERRA-2; Gelaro et al. 2017) and the NCEP Climate Forecast System, version 2 (CFSv2; Saha et al. 2014). These wind datasets provide data on global grids with size between 0.2° and 0.625°, and hourly temporal resolution.

2.3 Hydrodynamic model

The hydrodynamic and sediment transport modeling was performed with the Delft3D-FLOW module. Delft3D-FLOW simulates two-dimensional and three-dimensional hydrodynamic flows and transport phenomena over a domain driven by ambient forces. This module solves the unsteady non-linear shallow water equations under hydrostatic and Boussinesq approximations (Deltares 2020a). Currents in the model can be induced by tides, wind, Coriolis forces, surface waves, pressure gradients and density gradients, among other physical processes. Delft3D-FLOW is widely employed in studies regarding coastal and estuarine environments (Baptistelli 2015; Mendes et al. 2021; Huff et al. 2022), and it has been validated by laboratory and field studies (Elias et al. 2001; Gerritsen et al. 2008).

Two simulation periods, i.e., 2012 and 2019, were considered for the Delft3D-FLOW model. Calibration and validation of hydrodynamics were done for 2012 because of tide gauge data availability. However, the period employed for outfall sediment transport modeling was 2019 since suspended solid concentrations of the outfall effluents were only known for that year.

The computational domain was prescribed as a two-dimensional structured curvilinear grid with variable spatial resolution between 36 m and 1014 m. Variable resolution allows for a more detailed simulation in areas of interest while not consuming excessive computer power in other areas, e.g., near the boundaries. In Delft3D-FLOW, a two-dimensional grid implies a depth-average simulation, which is

justified in the present study because Santos Bay and its outer coastal area are weakly and briefly stratified during both neap and spring tide regimes (Belém et al. 2007; Harari et al. 2008). Bed elevations for this grid were interpolated from the available topographic and bathymetric datasets. Figure 2 shows the domain definition and a detail of the grid over interpolated bathymetry. Since the grid was defined in Cartesian coordinates, an average latitude was set to get a uniform Coriolis force over the entire domain.

Water level boundary conditions in open ocean were specified via amplitudes and phases of 14 tidal constituents from the TPXO global tidal model (Egbert and Erofeeva 2002). These harmonic constants were downloaded and spatially interpolated along a total of 63 boundary sections in western, southern and easter boundaries (see Figure 2) using Delft Dashboard (Ormondt et al. 2020). Time-varying salinity and temperature conditions from HYCOM were also specified at open boundaries for 2012 and 2019.

Uniform wind forcing was applied for the model by providing time series of wind speed and direction at 10 m elevation. For the 2012 period, wind time series from Bertioga station presented significant gaps, so NCEP/DOE winds were utilized. For 2019, Bertioga station was used since it presented robust time series with hourly resolution, whereas NCEP winds were 6-hourly. Sensitivity analyses on available subperiods showed that both wind datasets produce similar hydrodynamic results, so the most complete dataset was selected for each period. Additionally, an air density of $1.15\,\mathrm{kg/m^3}$ was used for the wind stress formulation.

For modeling heat exchange at the free surface, the Murakami scheme (Murakami et al. 1985) was used. This heat flux model considers the absorption of incoming radiation as a function of depth, and, although developed for Japanese waters, it has been applied to coastal waters in other regions (e.g., Pokavanich et al. 2008; Alosairi et al. 2018; Arifin et al. 2020). Time series of uniform relative humidity, air temperature and net solar radiation from the NCEP/DOE Reanalysis were prescribed for the Murakami scheme in both 2012 and 2019.

Constant flows were prescribed for the 27 point discharges corresponding to their mean annual flows in 2012 and 2019. Outfall discharges were prescribed as monthly averages in a single grid cell according to available data for both simulation periods (see Figure 3). Constant salinity of 0.1 ppt and temperature of 20°C were set for all freshwater point discharges and outfalls.

Model calibration was done mainly by minimizing the difference in water level between model results and measurements at Praticagem Santos for 2012. Differences in currents, salinity and temperature between the model and the HYCOM node near Praia Grande were also taken into account. The calibrated model was validated against water level time series at Ilha das Palmas for 2012 and compared with currents, salinity and temperature time series at the HYCOM nodes near Santos and Guarujá. Major calibration parameters were the Manning's bottom roughness coefficient, the wind drag coefficient and the time step. Calibration was achieved with a Manning's coefficient of $0.02\,\mathrm{m/s^{1/3}}$ with a linear wind drag coefficient between 0.001 and 0.003 for wind speeds between 0 and $25\,\mathrm{m/s}$. The simulation time step was defined to be 1 minute.

For depth-averaged models, Delft3D-FLOW implements background eddy viscosity and diffusivity to account for momentum and solute mixing due to unresolved turbulent motion and shear dispersion (Deltares 2020a). Eddy viscosity and diffusivity are usually calibration parameters since they are flow-dependent properties, in contrast to their molecular counterparts, which are properties of the fluid. Given the lack of measurements of velocity and solute dispersion in the study area, calibration for those parameters was not possible. However, preliminary runs were performed to study the sensitivity of the model to background eddy viscosity and diffusivity in a range between $10^{-2}\,\mathrm{m^2/s}$ and $10^{2}\,\mathrm{m^2/s}$. Variations in viscosity and diffusivity did not have significant effects on the order of magnitude of suspended sediment concentration and deposition rate. Water level and velocity inside the Santos bay also showed low sensi-

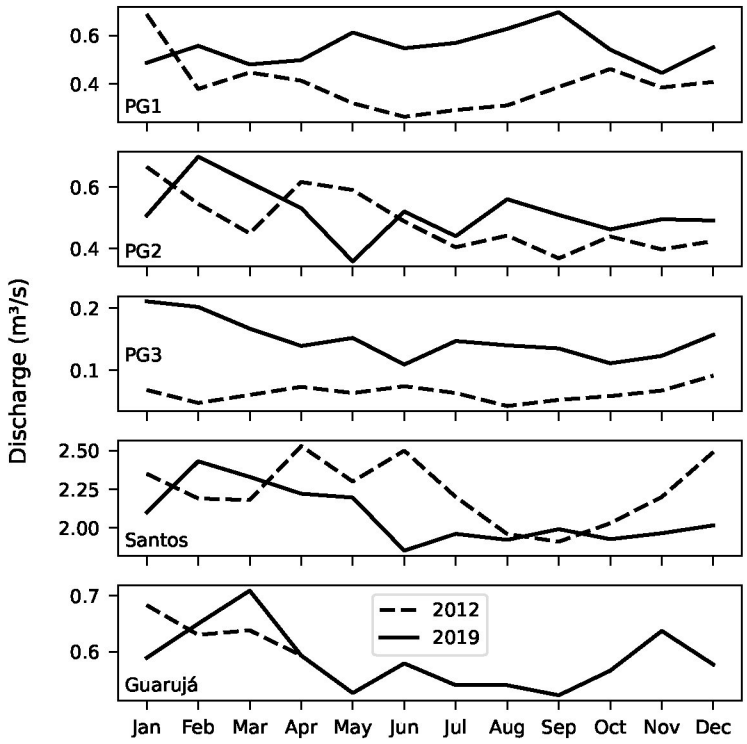

Figure 3: Average monthly discharges of the outfalls.

tivity to variations in eddy viscosity and diffusivity. Then, it is reasonable to assume that uncertainties in unresolved flow features (i.e., turbulence and shear dispersion) do not phenomenologicaly invalidate the conclusions of the present research. Finally, both background horizontal eddy viscosity and diffusivity were set to a uniform value of $1\,m^2/s$.

2.3.1 Sediment transport modeling

The suspended sediment concentrations in outfall discharges were estimated from analyses of total suspended solids of the outfall effluents in 2019. Constant total sediment concentrations were estimated to be $0.278\,kg/m^3$ for Santos outfall, $0.128\,kg/m^3$ for Guarujá outfall and $0.134\,kg/m^3$ for the three outfalls at Praia Grande. The grain size distribution was determined by laser diffraction granulometry of solids of a wastewater sample from the Santos treatment plant in March 2016 (Consórcio Partner/TetraTech 2017). The median grain size of the whole sample was $20\,\mu m$, showing that the effluent solids are mainly silt-sized. Given that the minimum median grain diameter accepted by Delft3D for non-cohesive sediment is $100\,\mu m$, the total suspended solids were divided into cohesive and non-cohesive fractions (see Figure 4a). For the non-cohesive fraction, the median size of $100\,\mu m$ was found in the upper 18% of the grain size distribution ($>62.4\,\mu m$). The lower 82% is then considered as cohesive sediment with a median size of $14.7\,\mu m$. The concentrations of suspended solids were split accordingly for each outfall.

By default, Delft3D uses a particle density of $2650\,kg/m^3$, typical of mineral sediments. However, since wastewater effluents usually contain a significant fraction of lighter organic particles ($1250\,kg/m^3$ on average; Boyd 1995), the default specific density must be corrected. Laboratory analysis of wastewater samples from the Santos treatment plant in 2015 (Figure 4b; Consórcio Partner/TetraTech 2017) shows that on average suspended solids are 81% volatile (organic) and 19% fixed (mineral). Following Avnimelech et al. (2001) and considering 81% and 19% of organic and mineral content, respectively, a

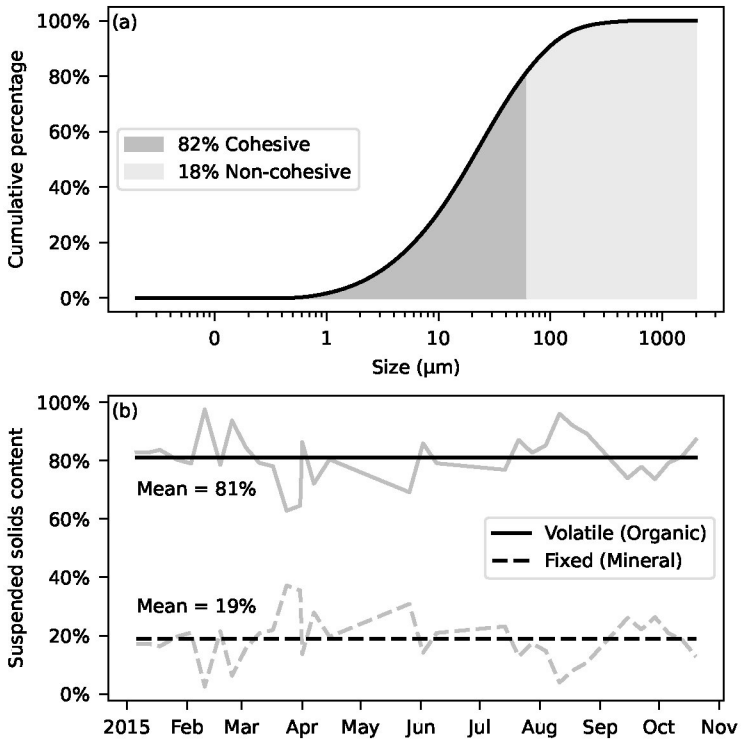

Figure 4: Granulometry (a) and composition (b) of effluent solids from the Santos treatment plant (Consórcio Partner/TetraTech 2017).

weighted average specific density of 1513 kg/m^3 was computed. Since dry bed density of the effluent solids was not available, it was estimated from the weighted specific density and the default porosity considered by Delft3D (81% and 40% for cohesive and non-cohesive sediments, respectively). Then, the bed dry densities were specified as 286 kg/m^3 for the cohesive fraction and 914 kg/m^3 for the non-cohesive fraction. Sediment dynamics of cohesive sediment depends on several other factors such as the settling velocity, salinity-induced flocculation and empirical parameters for sedimentation and erosion. However, these parameters were not available for the present study, so Delft3D defaults were used.

In order to analyze the transport and fate of sediment exclusively from the outfalls, initial sediment concentration and bed sediment layer were set to zero, and all other sources of sediment were disabled (i.e., concentration in point discharges and boundaries equal to zero).

2.4 Wave model

In order to simulate the propagation and evolution of wind-waves in the domain, the Delft3D-WAVE module was used. Delft3D-WAVE computes wave fields for given bathymetry, wind field and hydrodynamic conditions by running the SWAN model (Deltares 2020b). SWAN is a third-generation wave model that simulates the generation and propagation of wind-waves in coastal regions including shallow waters and ambient currents (Booij et al. 1999). SWAN is widely used for studies of waves in coastal environments, estuaries, tidal inlets and semi-enclosed basins (e.g., Lenstra et al. 2019; Rusu 2022; Iouzzi et al. 2022; Aydoğan and Ayat 2021), and it has been validated for a number of field and academic cases (Ris et al. 1999; Allard et al. 2004).

The mathematical description of waves in SWAN is fully spectral, so it accounts for random, short-crested wave fields. In random wave theory, the energy density spectrum describes the sea state at

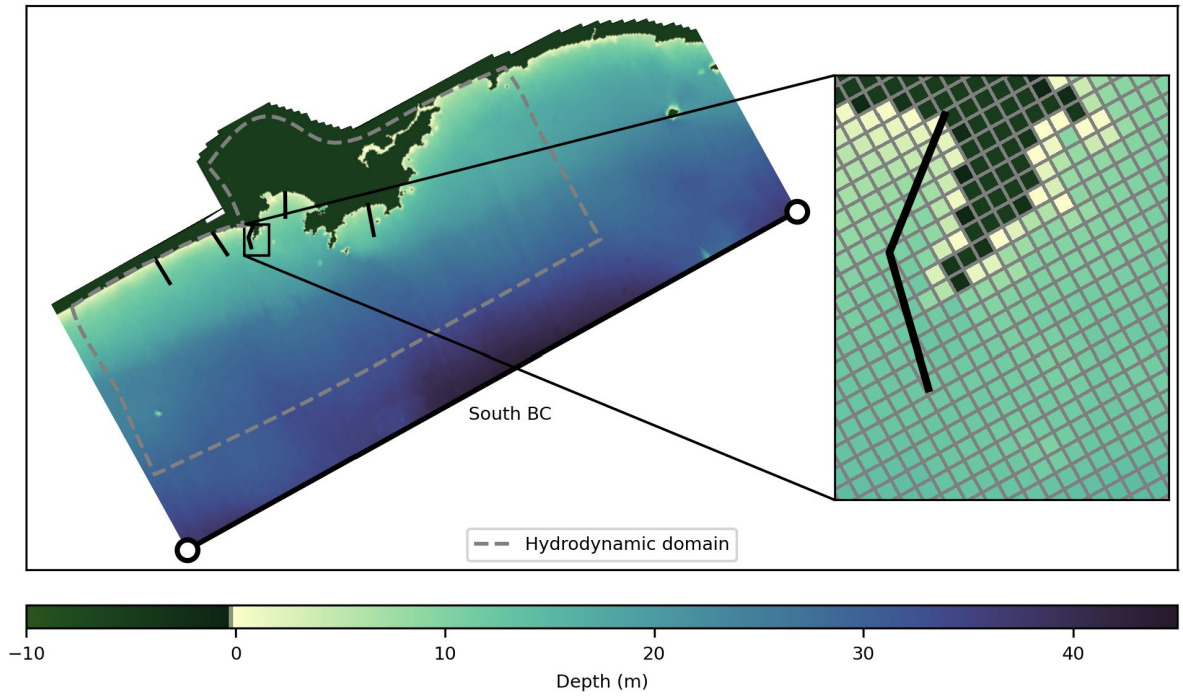

Figure 5: Delft3D-WAVE domain with interpolated bathymetry.

a certain location and time over a range of relative frequencies and propagation directions. Physical processes in deep, intermediate and shallow water dominate the evolution of this spectrum in space and time; however, SWAN adopts the action density spectrum because it is conserved during propagation under ambient currents, while the energy density spectrum is not (Komen et al. 1994; Whitham 1999).

For wave modeling, two periods were considered. The period for validation was 2016 due to availability of wave data from the buoy in Santos Bay. To study the influence of waves on outfall sediment transport, the period of 2019 was set up for wave-current coupling.

The wave domain was discretized as a structured grid with uniform resolution of 205 m and oriented along the hydrodynamic grid. The two-dimensional spectral space was discretized with 36 directions with a uniform 10° resolution and 24 frequency bins logarithmically distributed from 0.03 Hz to 1 Hz. In the same fashion as for the hydrodynamic model, bathymetry was interpolated from available surveys and datasets. Figure 5 shows the proposed wave model domain with the interpolated bathymetry and a detail of the grid. The computational domain of the wave model was defined to be larger than the hydrodynamic domain (see Figure 5) to simulate wave propagation from global hindcast nodes in deep waters (ERA5 and CAWCR). In practice, when a coupled simulation is performed, hydrodynamic and wave grids do not need to be identical since Delft3D can interpolate the required wave output to the hydrodynamic grid and vice-versa.

In the present simulation, the following processes were considered: energy input by wind; dissipation by bottom friction, depth-induced breaking and whitecapping; and non-linear wave-wave interactions, i.e., quadruplets and triads. By default, Delft3D-WAVE does not take into account triad interactions; however, they were activated due to their importance in redistributing wave energy over the spectrum in shallow water (Beji and Battjes 1993; Neill and Hashemi 2018). For bottom friction, Delft3D-WAVE applies by default the empirical JONSWAP formulation (Hasselmann et al. 1973) with a bottom friction coefficient of $0.067\,\mathrm{m^2/s^3}$, as proposed by Bouws and Komen (1983) for fully developed wind-sea conditions in shallow water. However, a more recent study by Vledder et al. (2011) shows that the value $0.038\,\mathrm{m^2/s^3}$

is applicable for a wide range of bottom materials and for both wind-sea and swell, so it is used in the present simulation.

Delft3D-WAVE requires the input wind speed to be at 10 m elevation although it actually uses the shear velocity for computations. SWAN employs an empirical drag coefficient to relate the 10-m wind speed to the wind shear velocity. For model input, space-varying and time-varying eastward and northward 10-m wind speed components were defined as subsets of the global atmospheric reanalysis grids, i.e., ERA5, CFSv2 and MERRA-2. Delft3D-WAVE interpolates the wind data internally to the computational grid.

Boundary conditions in Delft3D-WAVE can be specified as the product of a parametric one-dimensional spectrum and a directional distribution. By default, Delft3D-WAVE uses the JONSWAP spectrum (Hasselmann et al. 1973) that depends on the significant wave height and peak period, with a cosine-power distribution that depends on the mean wave direction and a power parameter (Deltares 2020b). Optionally, the directional spreading (standard deviation) can be provided instead of the power parameter since there exists a relationship between the parameters of the directional distribution and its statistical moments (Kuik et al. 1988). Following the default boundary condition parametrization in SWAN, time series of significant wave height, peak period, mean wave direction and directional spreading were generated from global wave datasets (ERA5 and CAWCR). In the present model, SWAN performs spectral interpolation between two support points to establish boundary conditions for all grid points along the southern boundary (see Figure 5).

The selection of appropriate wind field and wave boundary conditions was conducted by cross validation, i.e., testing a total of six different combinations of wind and wave datasets and comparing model results with significant wave height and peak period time series from a buoy in Santos Bay. The wind datasets considered were ERA5, CFSv2 and MERRA-2, while the wave datasets were from ERA5 and CAWCR. The best wave boundary condition and wind datasets were from CAWCR and ERA5, respectively. This combination is consistent with results from other authors. For example, a study by Kaiser et al. (2022) showed that ERA5 winds produce better results than CFSR for spectral wave modeling in the South Atlantic Ocean. Furthermore, the combination of CAWCR wave boundary conditions with ERA5 wind have been found to provide slightly more accurate results for wave modeling in the southern Brazil nearshore (Bose et al. 2022). The combination of ERA5 winds with CAWCR wave boundary conditions was then used for the 2019 wave-current coupling.

Although the model was set up with input data for the entire year 2019, for convenience, the model runs were performed by sub-periods. According to the time scale of variations in the incoming wave conditions (CAWCR Wave Hindcast), the length for the sub-periods was specified to be a month. The time series of wave integral parameters of 2019 from a CAWCR node were analyzed to determine relevant modeling sub-periods. January, March and July of 2019 were selected being representative of mild, mean and strong wave regimes, respectively. This selection is consistent with regional wave climate, i.e., the austral summer (January) and winter (July) have the higher and lower wave heights (see Pianca et al. 2010). The time series of significant wave height from the westernmost CAWCR node in Figure 1 (24.4°S, 46.4°W) is presented in Figure 6 for the three selected sub-periods.

2.5 Wave-current interaction modeling

The effect of wave-current interaction on the transport and fate of outfall sediment was evaluated by comparing the results of the standalone hydrodynamic model with the coupled hydrodynamic-wave model for the three defined sub-periods. Coupling between Delft3D-FLOW and Delft3D-WAVE was done in

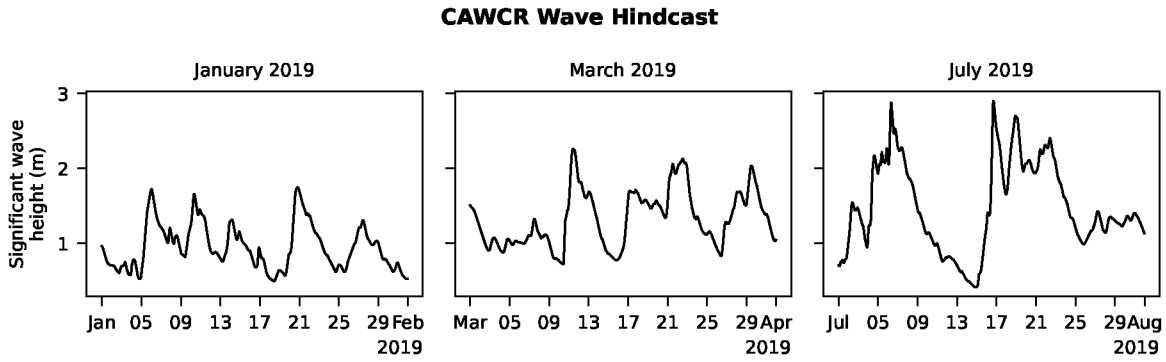

Figure 6: Time series of significant wave height from the western CAWCR node (24.4°S, 46.4°W).

online/dynamic mode. This mode allows for a two-way wave-current interaction in which both the effect of waves on currents and the effect of currents on waves are accounted for. Online coupling requires Delft3D to exchange flow and wave data through a communication file where the latest Delft3D-FLOW and Delft3D-WAVE results are stored. Delft3D-FLOW accounts for several wave-induced effects on hydrodynamics. Wave-induced forcing, Stokes drift and the enhancement of bed shear stress by waves have an overall effect over the vertical and can be considered in a depth-averaged form suitable for 2D computations, whereas streaming and wave-induced turbulence act at specific locations in the water column and can only be accounted for in 3D simulations (Deltares 2020a). The processes of wave-induced forcing, Stokes drift and bed shear stress enhancement considered in the present 2D hydrodynamic model are of major importance for coastal sediment transport and associated morphological evolution, and are discussed next.

Wave propagation is known to produce a net momentum flux on the mean flow, also called radiation stress, concept first developed by Longuet-Higgins and Stewart (1960). Radiation stress gradients induce forces that drive longshore currents, rip currents and cross-shore variations in water level known as set-up and set-down. Wave-driven longshore currents are of great importance for coastal sediment transport since they are closely related to littoral drift. However, as demonstrated by Longuet-Higgins (1972) and Battjes (1974), at least some dissipation by breaking is necessary for waves to drive mean currents; otherwise, stress gradients would be balanced by the associated changes in water level. This shows that the effect of radiation stresses on the mean flow is significant in the surf zone. Furthermore, Dingemans et al. (1987) showed that numerical differentiation of the radiation stress tensor can result in unrealistic currents, and a formulation in terms of wave energy dissipation would be more accurate. On this basis, Delft3D-FLOW implements wave forcing in terms of dissipation rates by bottom friction, breaking and whitecapping (Deltares 2020a).

Although fluid particles in surface waves describe a periodic backwards-forwards motion, they present a net horizontal displacement in the direction of wave propagation known as Stokes drift (Stokes 1847). Since linear wave theory predicts that particle trajectories are closed ellipses, this small net motion represents a non-linearity and can be defined as the difference between Lagrangian and Eulerian wave-averaged velocities (see Bremer and Breivik 2017; Bühler 2014). As shown by several authors, Stokes drift plays a role in net sediment transport in coastal waters (Longuet-Higgins 1953; Nielsen 1992; Vittori and Blondeaux 1996; Deigaard et al. 1999). In Delft3D, the total mass transport induced by Stokes drift is computed using the approach by Dean and Dalrymple (1991) and then added to the wave-averaged mass continuity equation (Deltares 2020a).

Wave and current bed boundary layers are dominated by turbulence generation, so they interact

non-linearly, causing the resultant bed shear stress to be higher than the simple addition of the shear stress due to waves and the shear stress due to currents (Soulsby and Humphery 1990). The non-linear boundary layer interaction results in time-mean and maximum components of oscillatory bed shear stress that are important drivers for sediment transport. Sediment resuspension is dominated by the maximum bed shear stress, while overall current velocity and diffusion of suspended particles are controlled by the time-mean bed shear stress. Numerous analytical and numerical methods exist to describe the combined boundary layer; however, Soulsby et al. (1993) developed a standard general parametrization for them, having each model its own set of fitting parameters. Delft3D-FLOW implements this parametrization for nine options of wave-current boundary layer models (Deltares 2020a). In the present work, the boundary layer interaction model by Fredsøe (1984) was specified.

A detailed description of the wave-current interaction mechanisms implemented in Delft3D-FLOW can be found in its user manual (Deltares 2020a). For a comprehensive review on wave-current interactions, see Zhang et al. (2022).

3 Results and discussion

3.1 Calibration and validation

Hydrodynamic and wave model accuracy was evaluated using the statistical index of model performance by Willmott et al. (2011),

$$d_{\mathrm{r}} = \begin{cases} 1 - \dfrac{\sum_{i=1}^{n} |P_i - O_i|}{c \sum_{i=1}^{n} \left| O_i - \bar{O} \right|}, & \sum_{i=1}^{n} |P_i - O_i| \leq c \sum_{i=1}^{n} \left| O_i - \bar{O} \right|, \\ \dfrac{c \sum_{i=1}^{n} \left| O_i - \bar{O} \right|}{\sum_{i=1}^{n} |P_i - O_i|} - 1, & \sum_{i=1}^{n} |P_i - O_i| > c \sum_{i=1}^{n} \left| O_i - \bar{O} \right|, \end{cases}$$

where P_i and O_i $(i = 1, 2, ..., n)$ are model predictions and pair-wise-matched observations, respectively; $\bar{O}$ is the mean of the observations; and $c = 2$. It is piecewisely defined so that it is bounded between -1.0 and 1.0. Index values near 1.0 indicate that the mean absolute error (MAE) is insignificant compared to the sum of the mean absolute deviations (MAD) about $\bar{O}$ of perfect-model predictions (the case where $P_i = O_i$) and observations (O_i), i.e., MAE/(2 MAD) ≈ 0.

A comparison between calibrated and observed water levels at Praticagem Santos is presented in Figure 7a,b. Calibration of the hydrodynamics was achieved up to a Willmott's index of 71% for the period July-December 2012. This shows an overall good agreement between modeled and observed water levels at the entrance of the Santos estuarine channel. Model validation against water level observations at Ilha das Palmas resulted in a Willmott's index of 72% for the period May-November 2012 (see Figure 8a,b). Water level at Ilha das Palmas is considered to be representative of the outer bay, so an overall good agreement was achieved for the inner and outer regions of Santos Bay. Also, scatter plots in Figures 7c and 8c show a fairly high positive correlation that supports model performance in terms of water level.

It is worth noticing that water level observations in Figures 7a and 8a present some events of significant deviations from the astronomical tide. These variations are generally produced by cold fronts and associated fluctuations of wind and atmospheric pressure. Extreme events such as storm surges also

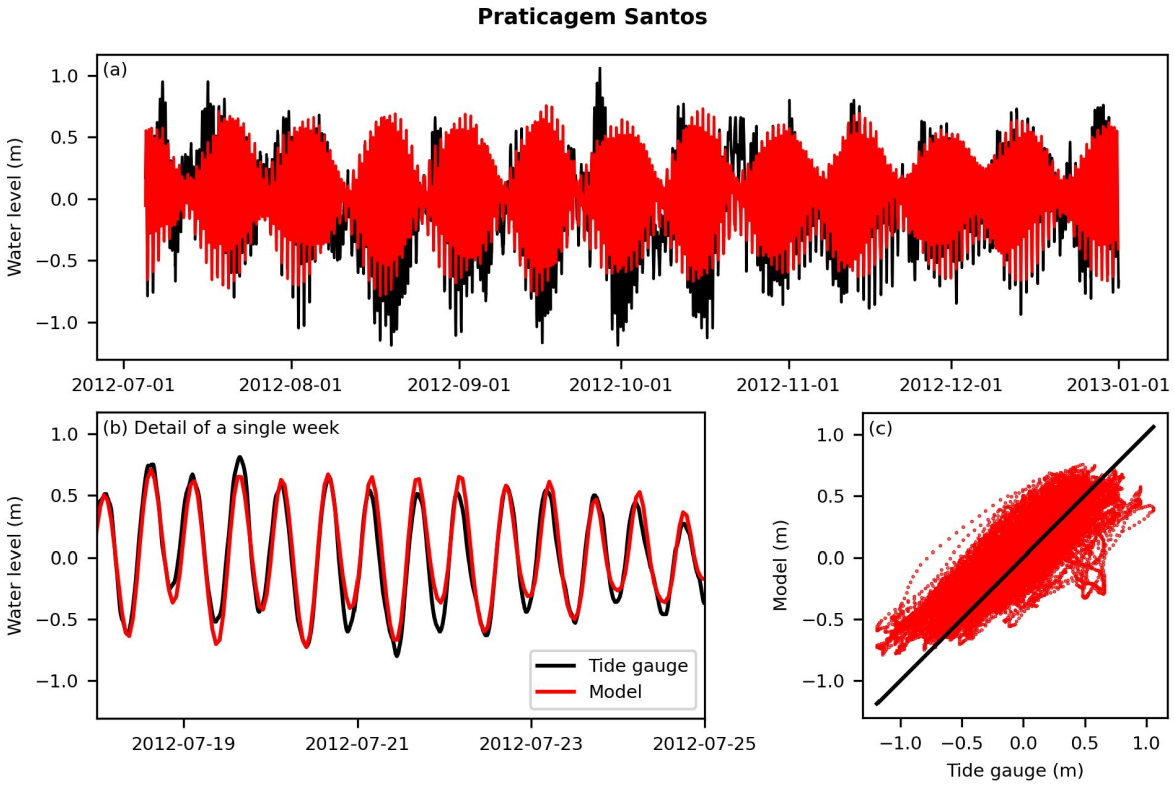

Figure 7: Water level time series (a, b) and scatter plot (c) at Praticagem Santos.

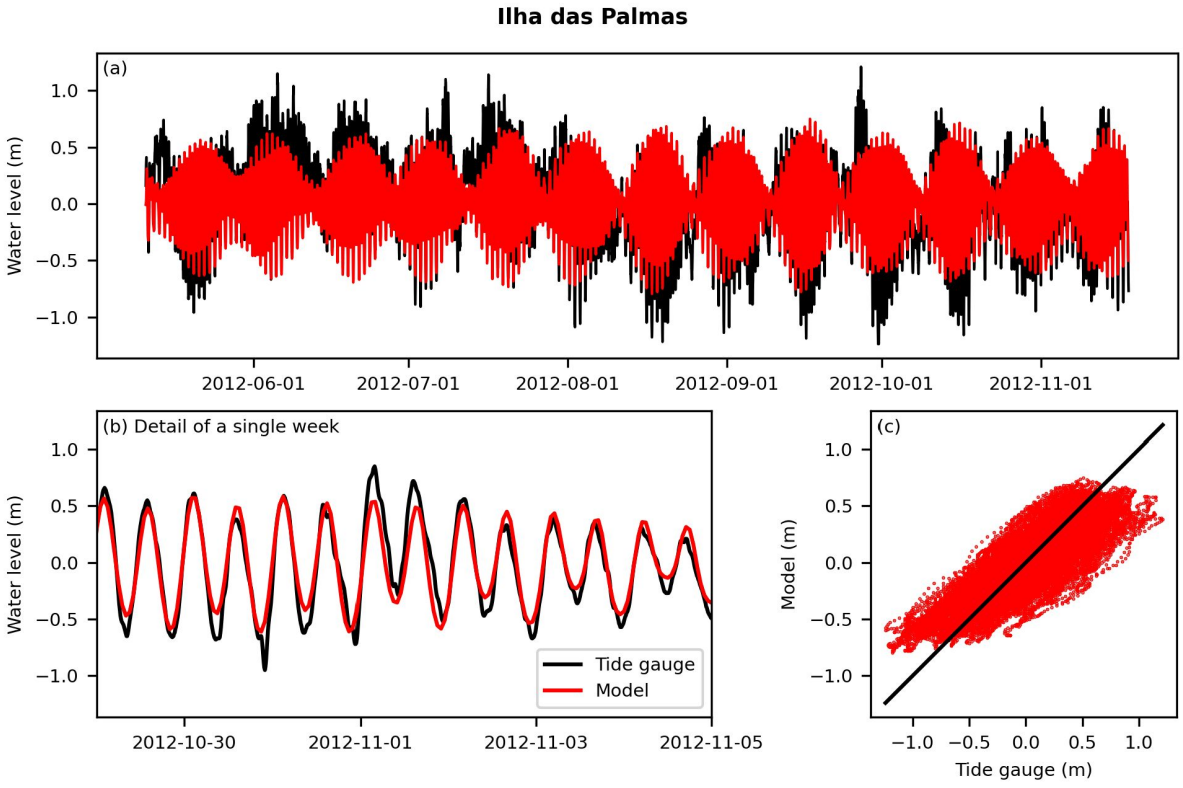

Figure 8: Water level time series (a, b) and scatter plot (c) at Ilha das Palmas.

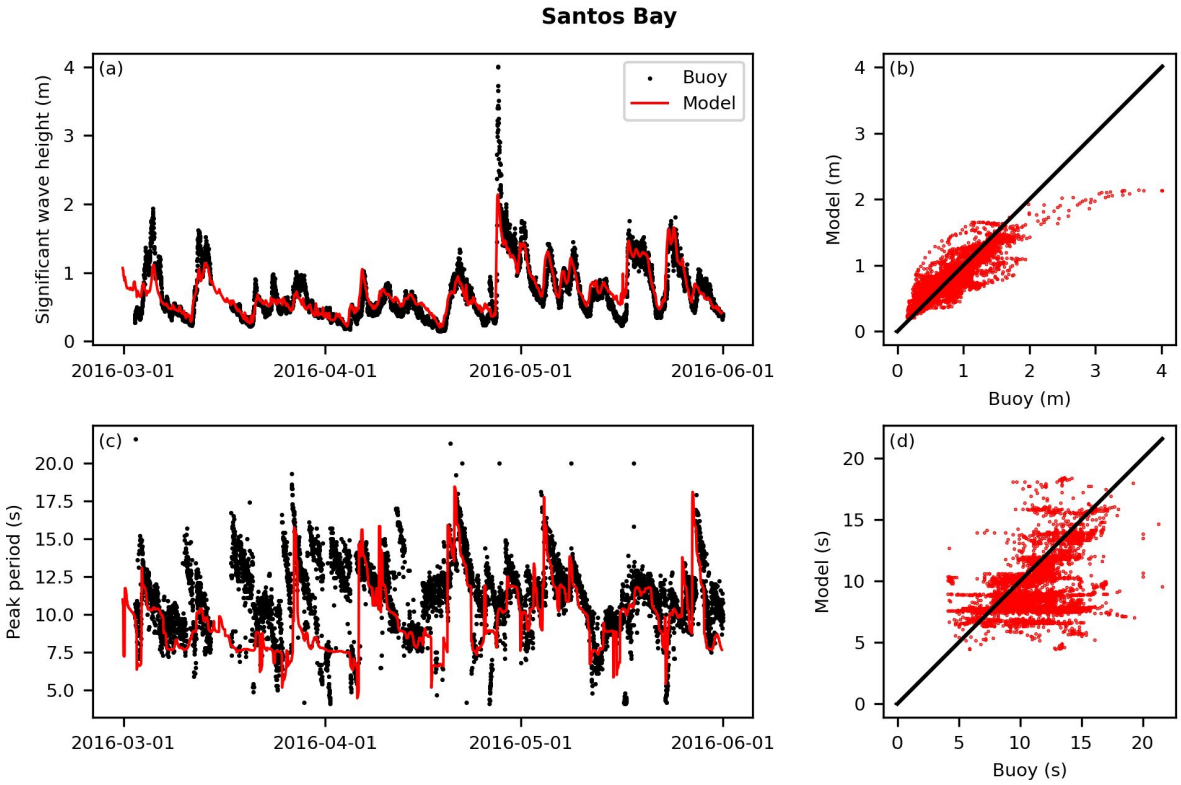

Figure 9: Time series and scatter plots of significant wave height (a, b) and peak period (c, d) in Santos Bay.

explain strong deviations in water level at the tide gauges. However, the influence of meteorological conditions and extreme events in submarine outfall plumes is out of the scope of the present study, so the hydrodynamic model was forced only with astronomical constituents at the open ocean boundaries.

The wave model was validated against wave time series from the buoy in Santos Bay. A comparison between modeled and observed significant wave height and peak period can be found in Figures 9a and 9c, respectively. Willmott's index for significant wave height results was 78%, showing an overall good agreement with observed waves in the period March-May 2016. However, on April 27 the buoy recorded an event with significant wave heights of up to 4 m that was not reproduced by the model. These wave heights were also not observed in ERA5 and CAWCR boundary condition data. A possible explanation for the peak may be extreme conditions underestimated by global wind and wave reanalyses (see, e.g., Stopa 2018).

With respect to peak wave period, significant deviations were found, and the overall model performance index was 43% for March-May, indicating reduced agreement. Nevertheless, from mid-April onwards, the modeled peak period becomes qualitatively more accurate, and the Willmott's index has a mild improvement, reaching 56% for the period from April 20 onwards. Model performance in terms of peak period will be considered to be acceptable. However, given that the observed peak period time series is significantly noisy, and no outlier filtering was applied, the performance of the model with respect to significant wave height will be considered to be more representative.

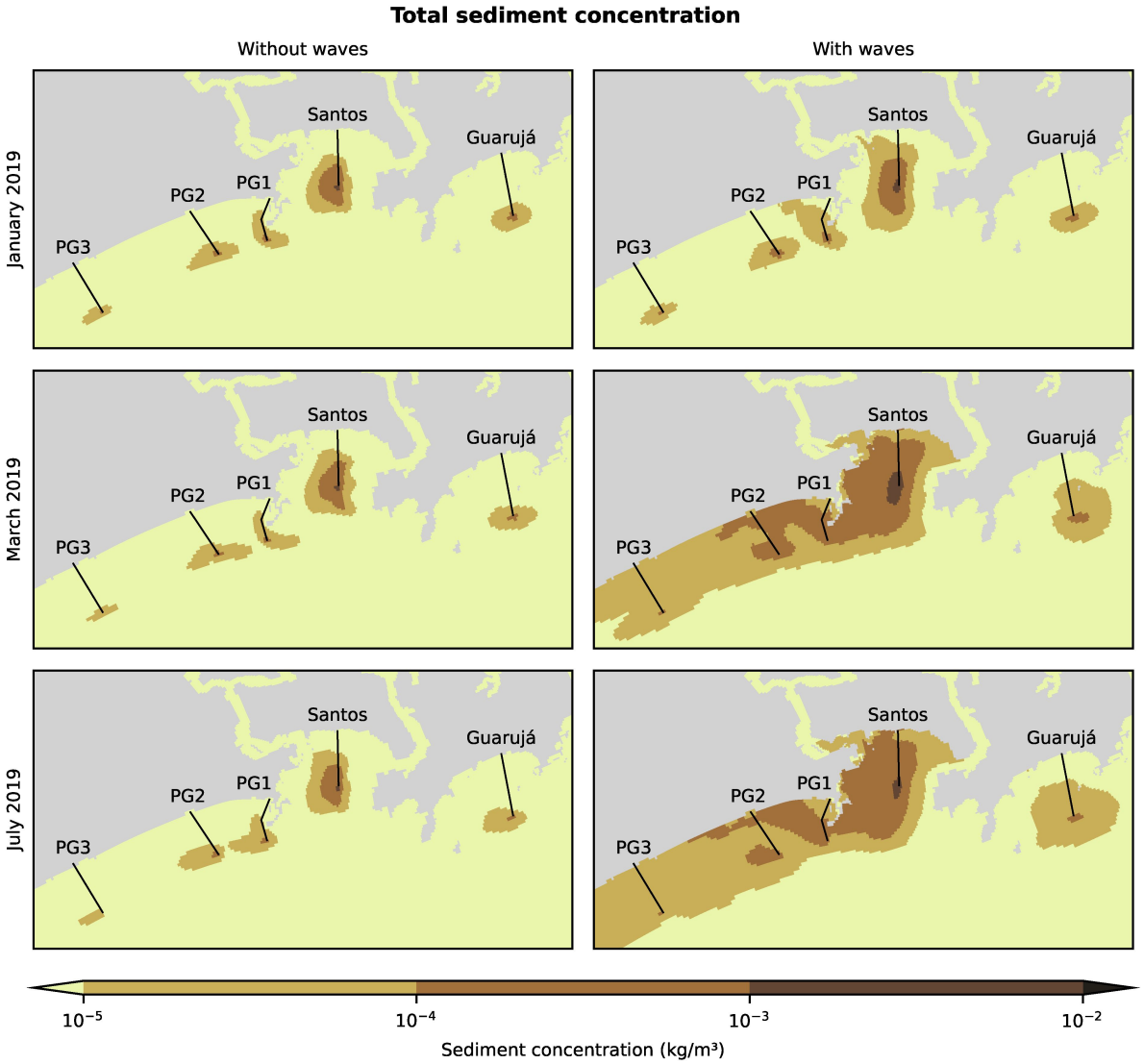

Figure 10: Temporal mean of total sediment concentration with and without waves.

3.2 Sediment transport

The sum of the cohesive and non-cohesive fractions was computed to give the total sediment concentration in the water column. Since this quantity is highly variable over time, being dominated by the outfall plumes, the temporal mean of each cell was calculated along the domain. Figure 10 shows a comparison of the time-mean total sediment concentration between the current-only hydrodynamic model and the coupled wave-current model for the three sub-periods (January, March and July 2019). It can be observed that, among the five submarine outfalls, the outfall in Santos Bay has the largest sediment plume for all the sub-periods. This result is expected because the Santos outfall has the highest discharge and the highest concentration of total suspended solids (see Figure 3 and Section 2.3.1). Interestingly, under the influence of waves, all outfalls exhibit more dispersed plumes, reaching higher concentrations in areas where sediment would be on average more diluted under the no-waves condition. This effect is more pronounced with mean and strong wave conditions (March and July). Since the effluent discharges and the suspended solids concentrations are kept constant between current-only and wave-current scenarios, this phenomenon must be associated with wave action.

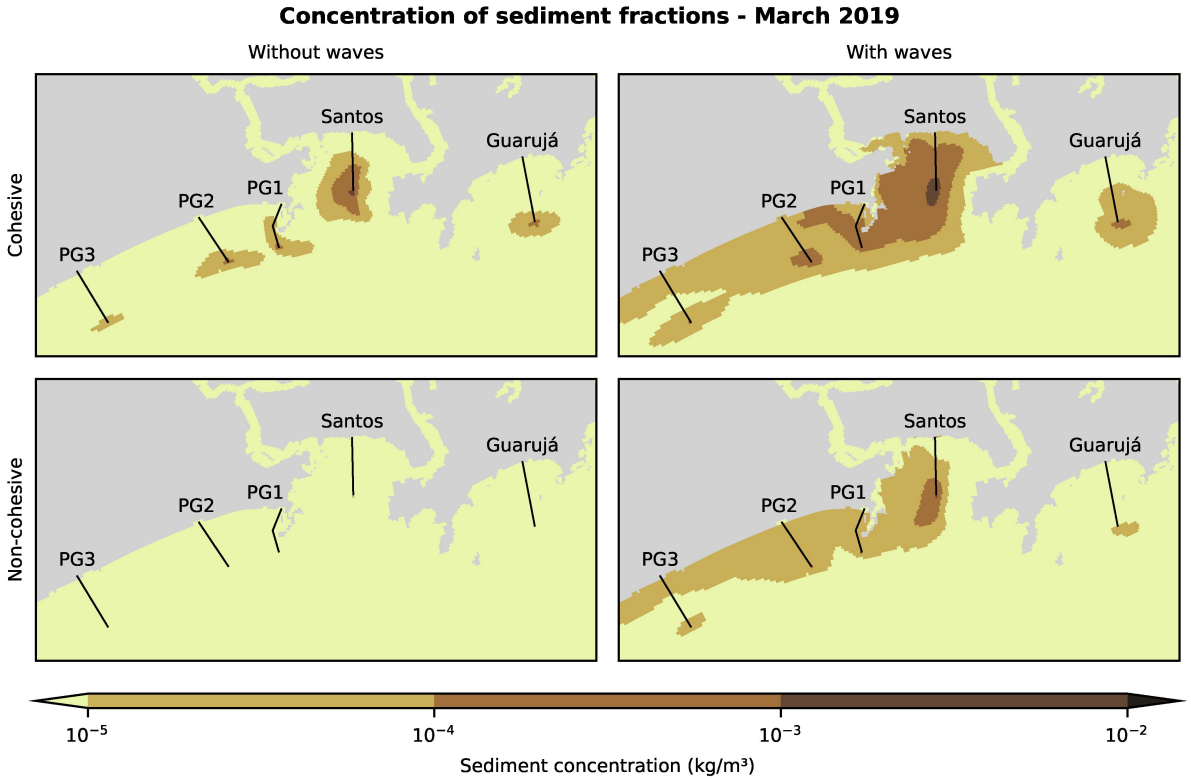

Figure 11: Temporal mean of sediment concentration for cohesive and non-cohesive fractions (with and without waves).

The extension of the sediment plumes under the influence of waves is not surprising. As illustrated by Magris et al. (2019), sediment discharges from land-based activities can produce plumes of fine-grained sediment that extend up to hundred of kilometers from the release point, reaching nearby shores. This is reasonable given the conservative nature of sediment as a constituent. However, due to settling and dilution, the discharged sediment can rapidly reach concentrations below reference ambient levels, perhaps posing negligible impacts on the environment. In fact, suspended solids in the outfall effluents are $\mathcal{O}(10^{-1}\,\mathrm{kg/m^3})$ and, after release, get rapidly diluted up to $\mathcal{O}(10^{-3}\,\mathrm{kg/m^3})$ and lower, which is below ambient concentrations, i.e., $\mathcal{O}(10^{-2}\,\mathrm{kg/m^3})$ (Berzin 1992).

The contribution of cohesive and non-cohesive sediment fractions to the total sediment concentration is shown in Figure 11 for mean wave conditions, i.e., March 2019. It can be observed that the cohesive fraction dominates the total sediment concentration (Figure 10). This occurs by two main reasons reasons. First, cohesive sediment constitute 81% of the total sediment concentration in the effluents. Second, due to its fine-grained nature, cohesive particles take more time to settle than non-cohesive sediment. The latter allows the particles to be transported further from the discharge location before intercepting the seabed.

The mass of cohesive and non-cohesive sediment deposited at the seabed is presented in Figure 12, also for March 2019 (mean wave conditions). Deposition for both fractions appears to be consistent with the corresponding plumes in Figure 11. For example, without the influence of waves, non-cohesive sediment rapidly settles in a small area around the diffuser for all five outfalls, producing negligible concentrations in the water column (of the order of $10^{-5}\,\mathrm{kg/m^3}$ and lower; see Figure 11). The cohesive fraction, however, gets more initial dispersion, and most of the deposition occurs within 1–2 km from the diffusers. On the other hand, when considering the effect of waves, both fractions get highly more

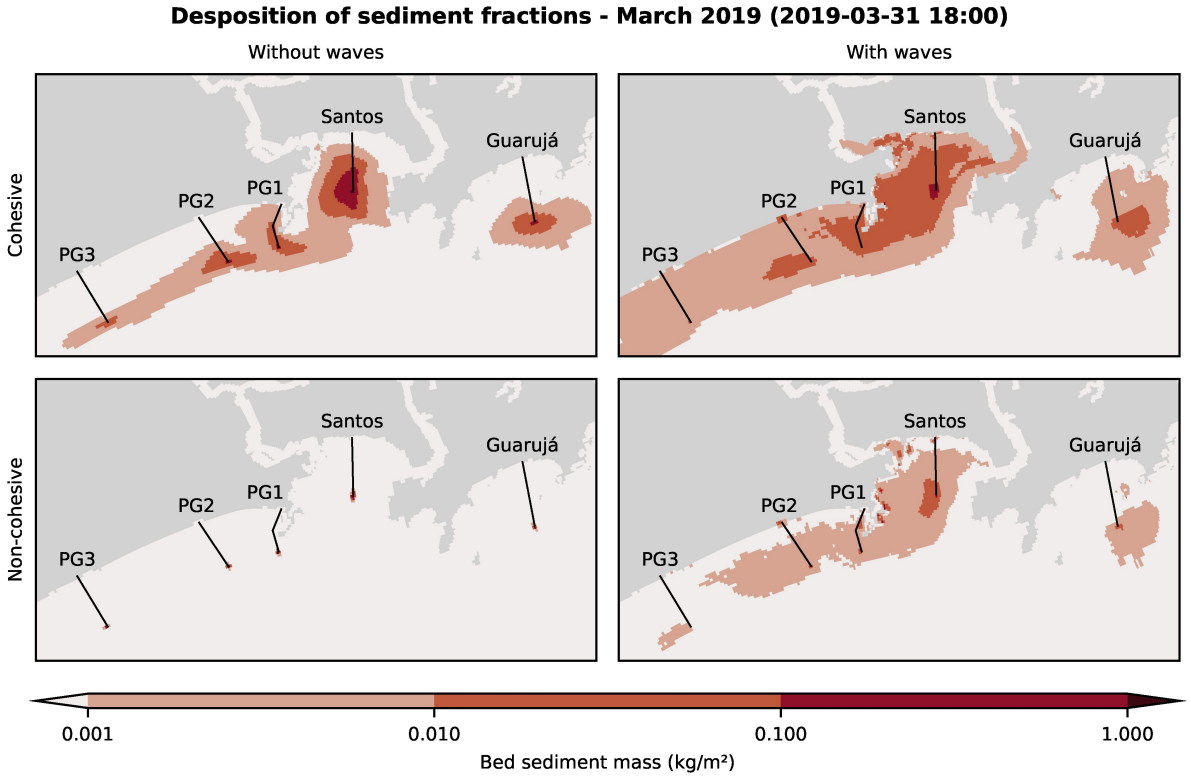

Figure 12: Sediment deposition at the end of March 2019, with and without wave influence.

dispersed over the domain. In particular, the non-cohesive fraction shows a drastic difference in plume extension, suggesting that wave action reentrains most of this sediment to the water column.

The deposited sediment mass (kg/m^2) was converted to sediment layer thickness (m) using the dry densities of cohesive and non-cohesive fractions. Deposition quantities expressed in terms of thickness are more intuitive and easier to reason about than mass per area, so, in Figure 13, the bed sediment layer thickness for the three sub-periods is presented. From observing Figure 13, it is evident that waves play a significant role in outfall sediment dispersion, affecting the final geometry of the deposits at the end of the sub-periods. Under wave influence, outfall sediment is mobilized over greater distances from the discharge point, reaching the entrance of the estuarine channels of São Vicente and Santos, and the coasts to the west. This is consistent with sediment plumes in Figure 10, especially under mean and strong wave regimes, where sediment is transported by westerly longshore currents. The overall deposition in the Santos Bay is compatible with a sedimentation sector that Fukumoto et al. (2006) identified in the mid-western part of the bay and consists mainly of organic-rich facies. Indeed, Fukumoto et al. (2006) proposed the influence of the Santos submarine outfall as one of the factors associated to this deposition area.

The order of magnitude of the sediment layer thickness is also shown in Figure 13. Without the influence of waves, the Santos outfall produces a thicker bed sediment layer, up to $\mathcal{O}(1\,\mathrm{cm})$ in a small area in the vicinity of the diffuser, while the outfalls of Guarujá, PG1, PG2 and PG3 showed maximum depositions of $\mathcal{O}(1\,\mathrm{mm})$. The location of the peak thickness is in the vicinity of the diffuser for all five outfalls, and this behavior remains unchanged between the current-only and wave-current models. In the months of March and July, the order of magnitude of the sediment layer thickness is greatly influenced by wave action; the sediment becomes distributed over larger areas with a lower thickness.

Events of sediment resuspension were found while analyzing the evolution of the bed sediment layer

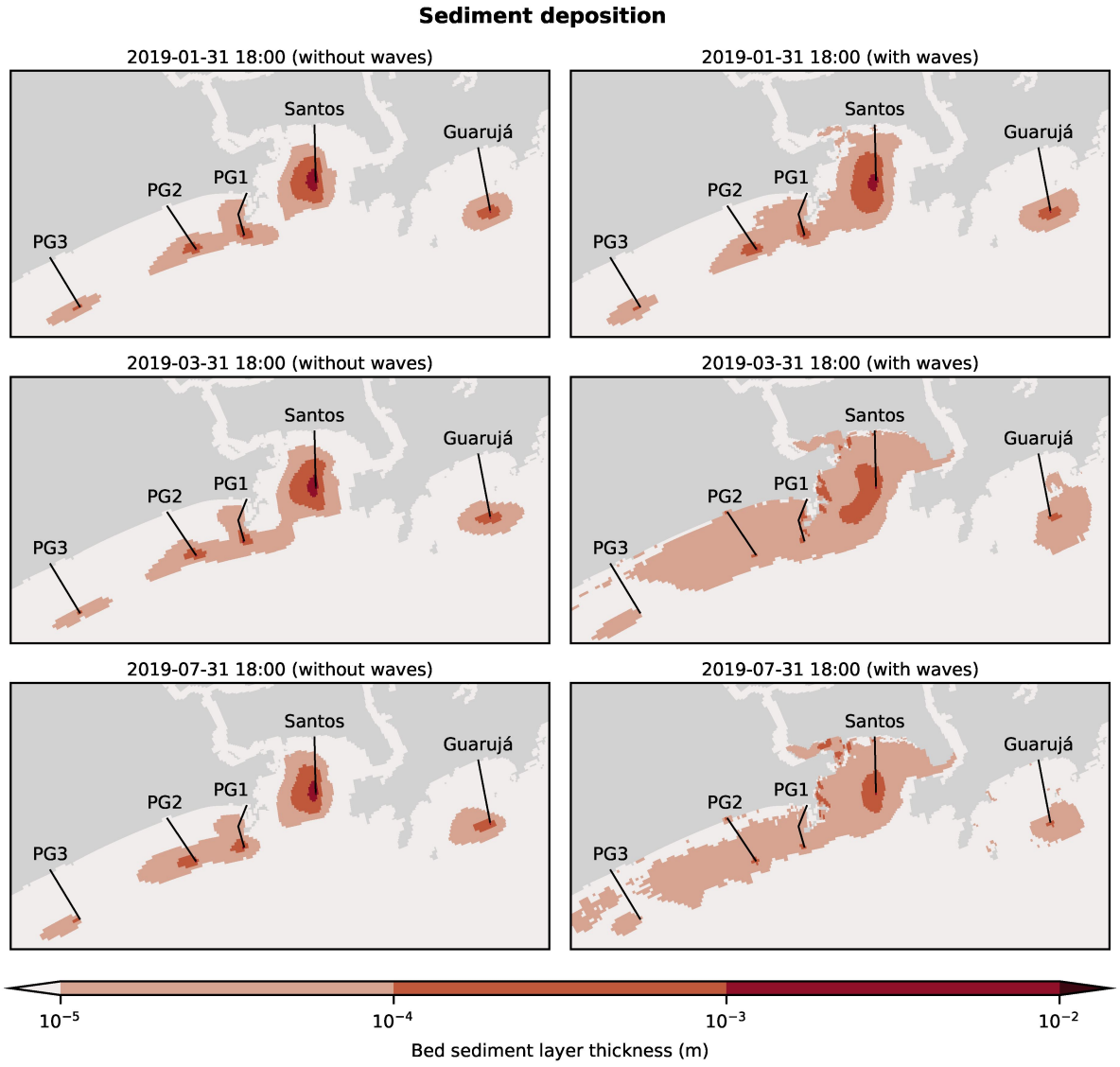

Figure 13: Sediment deposition at the end of the sub-periods, with and without wave influence.

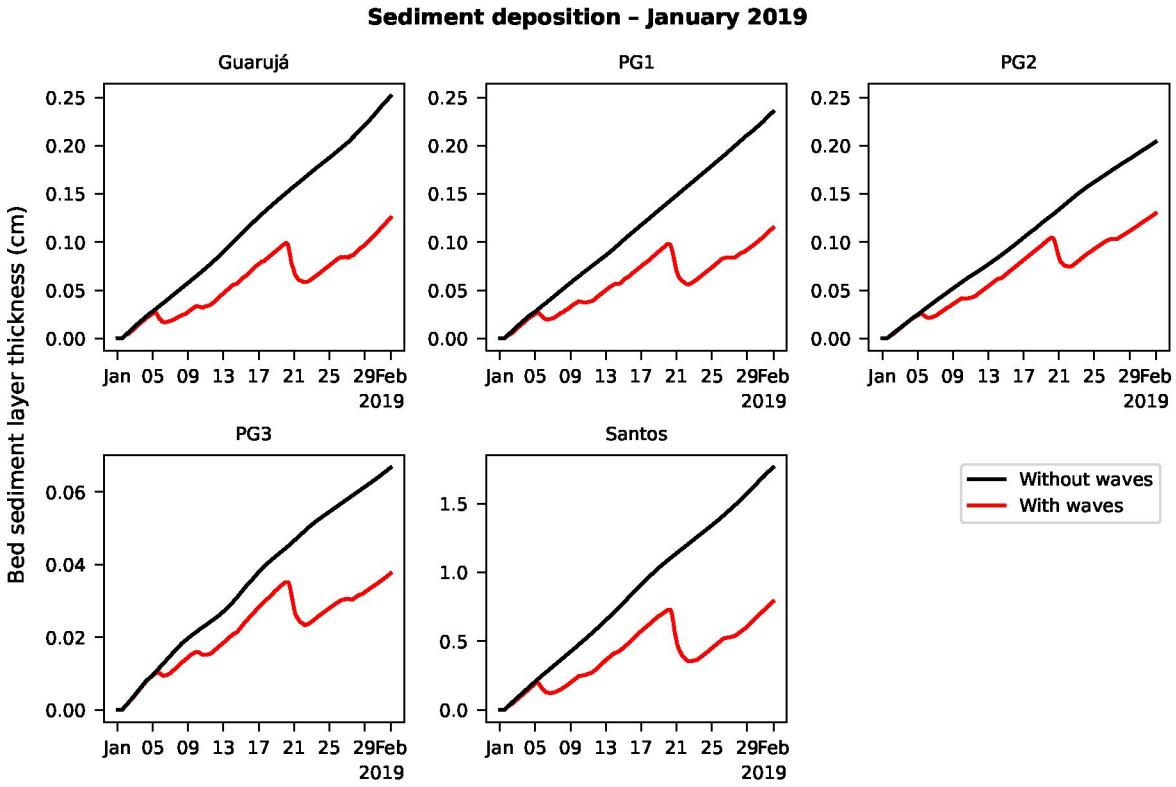

Figure 14: Evolution of the bed sediment layer in the vicinity of the diffusers in January 2019.

near the outfall diffusers (Figures 14 and 15 for mild and strong waves scenarios, respectively). Resuspension due to combined waves and currents occurs in the first and third weeks of January 2019, around days 5 and 20, for all outfalls (Figure 14). A less significant event of resuspension is observed on day 10. In July 2019, resuspension is more persistent, showing only a brief period of undisturbed deposition around the second week (Figure 15). The observed events of wave-generated resuspension can explain the increased sediment concentrations in the water column (Figure 10) because, once re-entrainment occurs, sediment is further transported by currents.

The outfalls of Santos and PG3 showed the highest and lowest final sediment deposition, respectively, coinciding with the magnitude of their discharges. Without wave effects, the Santos outfall produced a final deposition of 1.76 cm, and PG3 had only 0.07 cm at the end of January (mild wave conditions). However, if considering waves, sediment deposition suffers reductions between 36% and 55%. With waves, the final deposition in January 2019 for Santos resulted in 0.79 cm, and in PG3 it was about 0.04 cm. On the other hand, considering the strong wave action of July, the sediment layer in Santos drops from 1.59 cm to 0.16 cm (90%), and in PG3 it goes from 0.04 cm to 0.01 cm (83%). This supports a relationship between the strength of wave conditions and the amount of resuspension. Also, those differences in sediment layer thickness indicate that, due to the action of waves, a large part of the sediment is removed from the location of initial deposition, preventing continued accumulation. In general, it can be noted that the deposition patterns are consistent among the five outfalls; they all show similar trends of sedimentation and erosion, only varying in magnitude. So, for the sake of brevity, from now on, only results for the Santos outfall will be presented.

As observed in Figures 14 and 15, the undisturbed depositional trend is approximately linear. However, a detailed view of the deposition rate near the Santos outfall diffuser (Figure 16) shows that it has oscillation modes associated with the tidal motion. The average deposition rate is between 0.05 cm/day

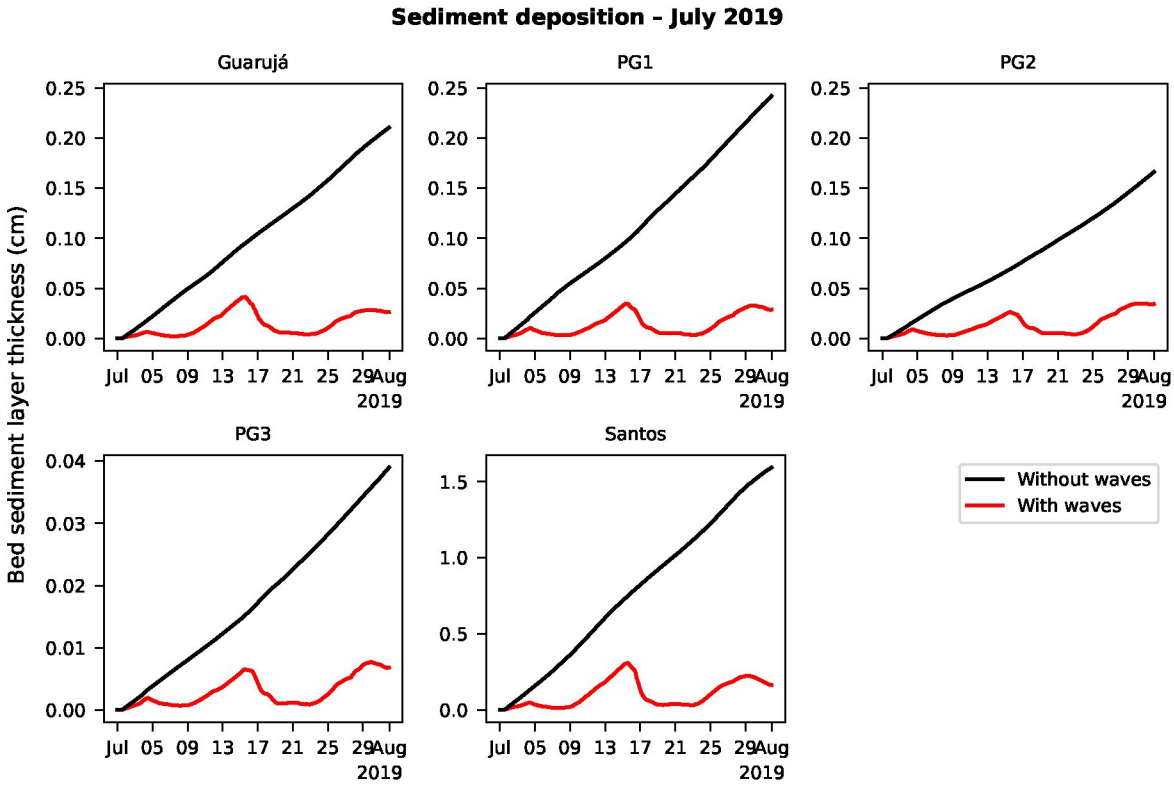

Figure 15: Evolution of the bed sediment layer in the vicinity of the diffusers in July 2019.

and 0.06 cm/day for the three sub-periods. At such accelerated rate, after a whole year, an undisturbed deposition would result in a sediment layer of about 20 cm. Due to wave action, deposition in the model is frequently hindered and interrupted, preventing the formation of unrealistic sediment deposits in the long term.

In periods of reduced wave action, the deposition rate (slope) under calm conditions is approximately the same between the standalone hydrodynamic model and the coupled wave-current model (see, e.g., January 2019 in Figure 16). Figure 16 also shows that after events of resuspension (rate below zero) the deposition process tends to regain the initial rate. This behavior suggests that, in the model, waves do not have a significant effect on the deposition rate per se and only cause temporary disruptions. Nevertheless, in March and July, wave conditions are strong enough to hinder deposition during most of the sub-period.

In the present model, outfall sediment transport take place over a fixed bed, and sediment resuspension is limited by the available outfall sediment at bed. For example, in January 2019, there is more time of undisturbed deposition, so the available *resuspendable* sediment is greater. That is why January 2019 show a more intense resuspension event than March and July 2019 (-0.6 cm/day; see Figure 16). Sediment resuspension also depends on the grain size distribution because sand-sized sediment is easier to resuspend due to its non-cohesive nature. For instance, since non-cohesive sediment tends to settle closer to the diffusers than cohesive sediment (as illustrated in Figure12), resuspension rates in the vicinity of the outfalls are controlled by non-cohesive sediment.

Since sediment resuspension is dominated by the bed shear stress, it is expected that the interaction of waves and currents induces higher stresses. As shown in Figure 17, the inclusion of waves in the hydrodynamic model produces a significant increase in bed shear stress. For example, around July 7, the shear stress in the standalone hydrodynamic model reached values of $\mathcal{O}(10^{-2}\,\mathrm{N/m^2})$ in the vicinity of the Santos outfall diffuser, but the presence of waves induced shear stresses of up to $\mathcal{O}(10^{-1}\,\mathrm{N/m^2})$.

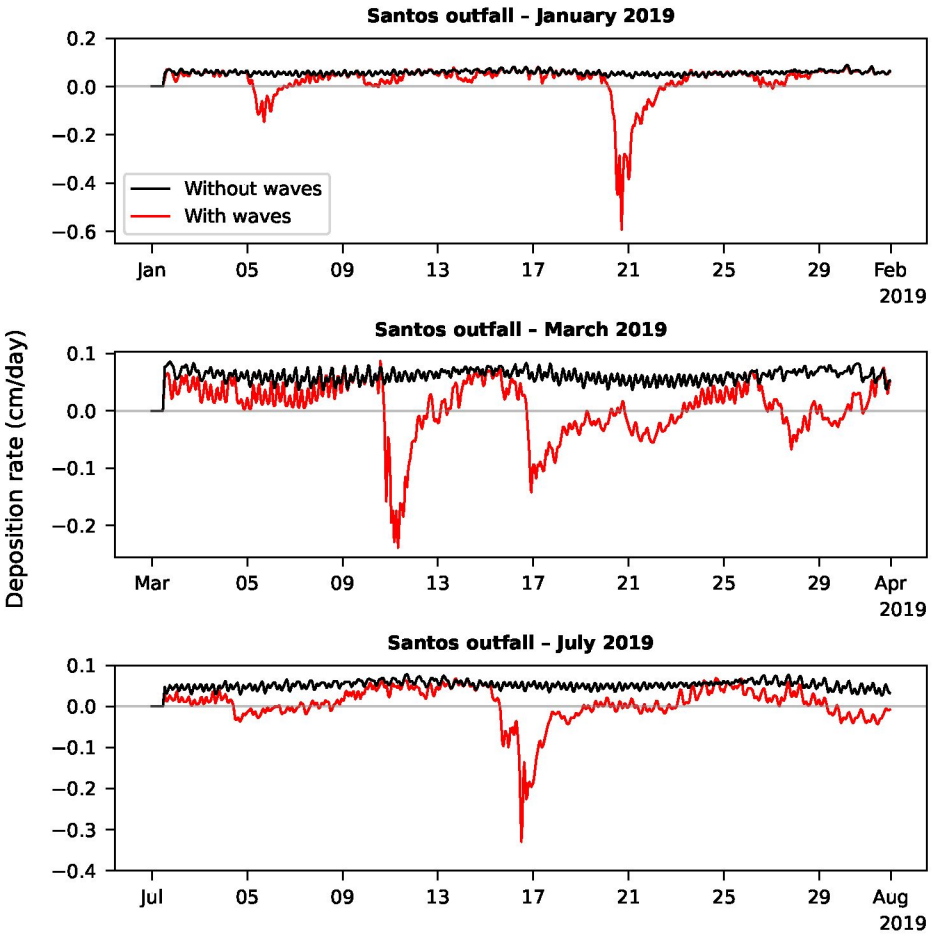

Figure 16: Deposition rate in the vicinity of the Santos outfall diffuser.

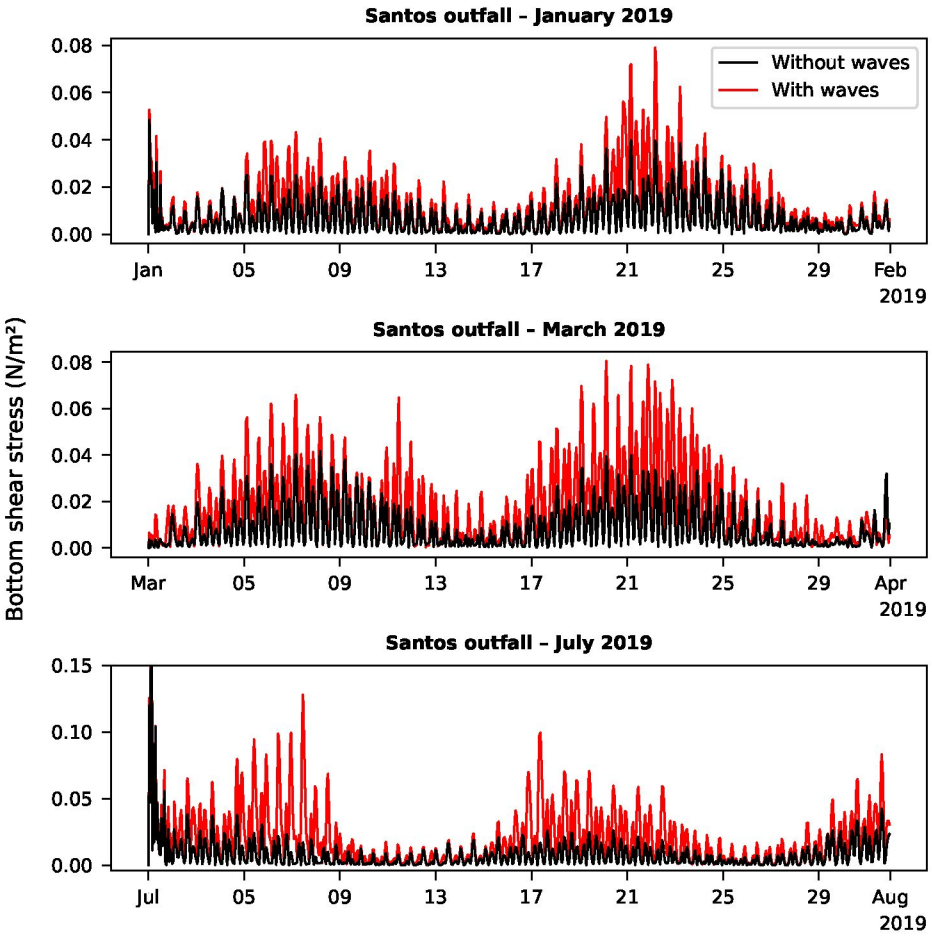

Figure 17: Bed shear stress in the vicinity of the Santos outfall diffuser.

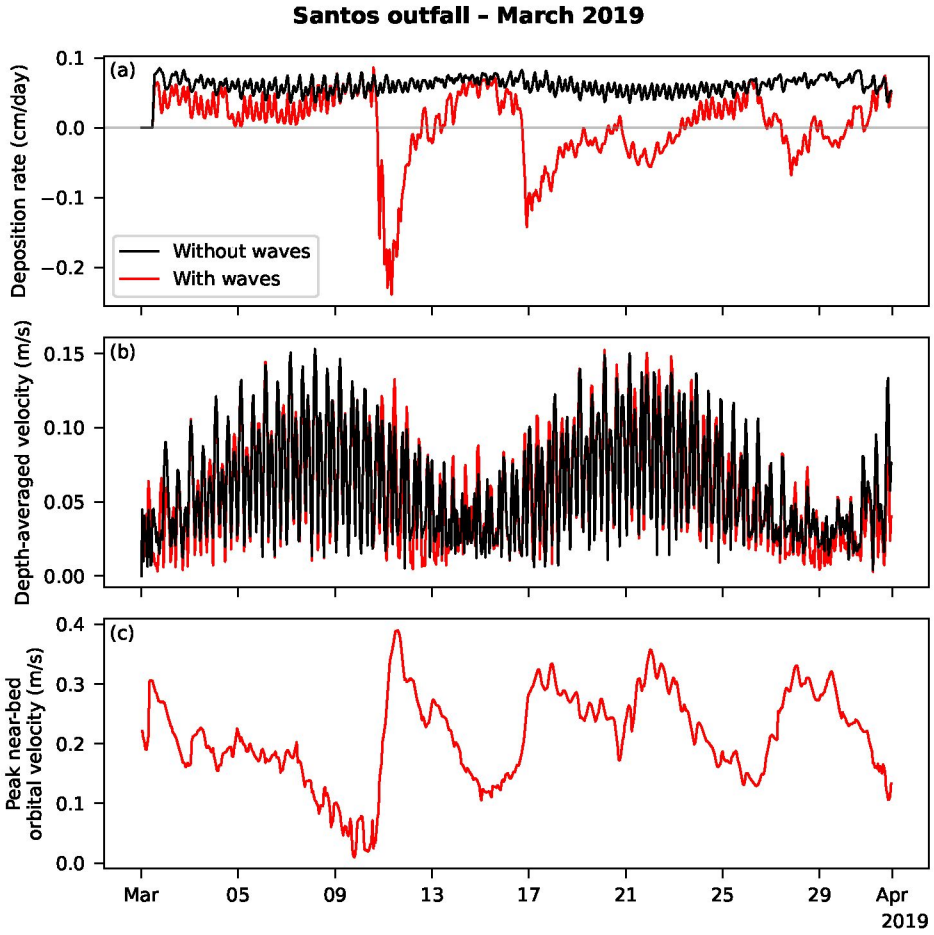

Figure 18: Deposition rate (a), depth-averaged velocity (b) and peak near-bottom orbital velocity (c) in the vicinity of the Santos outfall diffuser in March 2019.

The enhancement of bed shear stresses is produced by a non-linear combination of current and wave stresses, which results in time-mean and maximum components of oscillatory stress (Soulsby et al. 1993). Wave propagation can force currents, increasing their velocity and associated time-mean stress; however, waves themselves produce a progressive orbital motion that controls the maximum component of oscillatory stress. The contribution of those two mechanisms can be assessed by comparing the overall increase in current velocity due to the inclusion of waves and the near-bottom wave orbital velocity. Current velocities in Figure 18b are slightly affected by wave action because outfall diffusers are located offshore outside of the surf zone, in areas where radiation stresses are not able to drive significant currents. On the other hand, near-bed orbital velocities at the same location (Figure 18c) have pronounced peaks with higher magnitudes than those of currents. Strong near-bottom orbital motion can stir up bed sediments, producing the resuspension events observed in Figure 18a. This indicates that the dominant process for the enhancement of bed shear stress is the orbital motion of waves.

According to linear wave theory, the lower limit of wave action is at a depth equal to half the wavelength. Waves propagating over water deeper than this limit are deep-water waves. The effect of deep-water waves on the seabed is negligible; however, once the waves reach shallower depths, they begin to interact with the seabed. Figure 19 presents the depth-wavelength ratio of waves near the Santos outfall diffuser and the lower limit that corresponds to a ratio of 0.5. In January 2019, it can be seen that waves are in the deep-water regime most of the time with brief incursion into a transitional regime (<0.5)

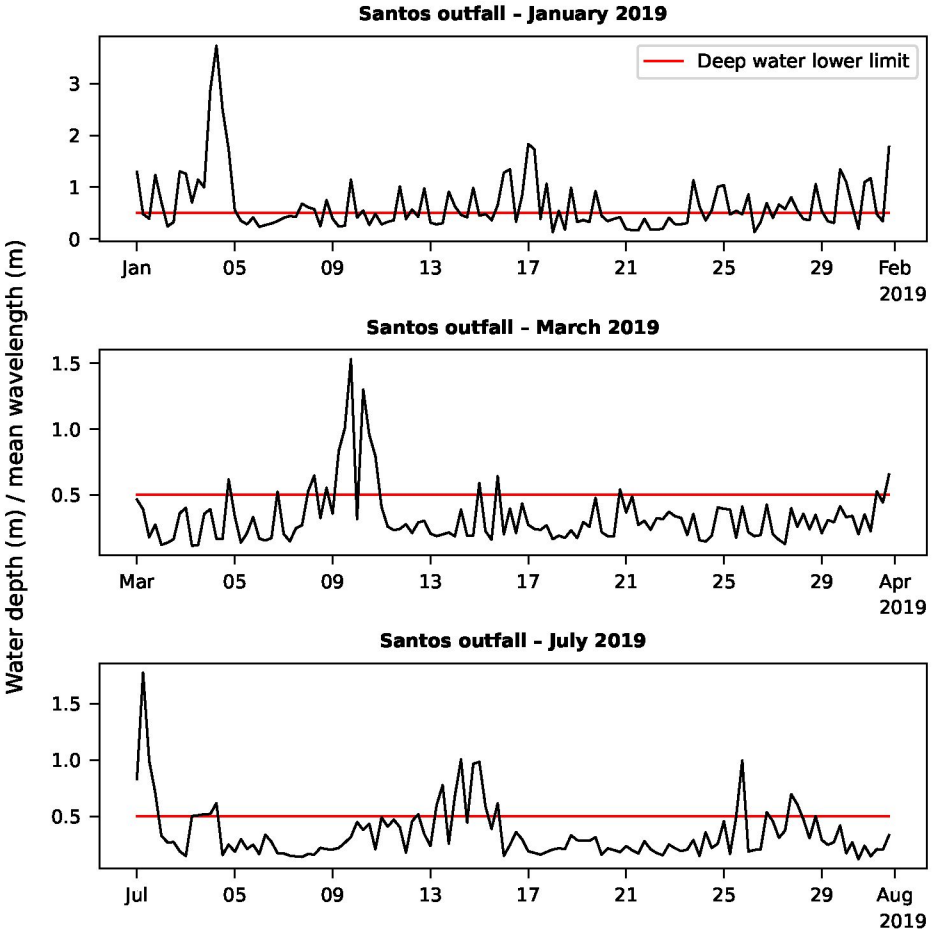

Figure 19: Depth-wavelength ratio in the vicinity of the Santos outfall diffuser.

in which near-bed elliptical motions can stir up bed sediment. On the other hand, in March and July, waves are mostly in the intermediate regime. Since March is representative of mean wave conditions, resuspension events and hindered deposition can be expected throughout most of the year.

As pointed out by Wiberg and Sherwood (2008), for linear waves, the near-bed orbital velocity is directly proportional to wave height, and its dependence on period and depth is subtler. This can be confirmed for Santos by observing Figure 20. In fact, for the depths at the outfall discharge points, time series of wave orbital velocity resemble those of significant wave height for all three sub-periods. Furthermore, by comparing the occurrence of resuspension events (negative deposition ratios) with wave conditions, it is found that resuspension can occur under significant heights as low as 0.57 m with mean periods of 5.5 s in January.

3.3 Outlook

Since sediment transport is a complex process, especially for fine and silt-sized sediments such as those found in the effluents, a more detailed model implementation could be beneficial. However, this would require additional laboratory analyses to determine settling velocity, salinity-induced flocculation and empirical parameters for sedimentation and erosion, as implemented in Delft3D (Deltares 2020a). Additionally, one could implement coupled water-sediment quality modeling, i.e., the interaction of wastewater pollutants with sediment particles. For example, taking into account sediment-attached fecal bacteria

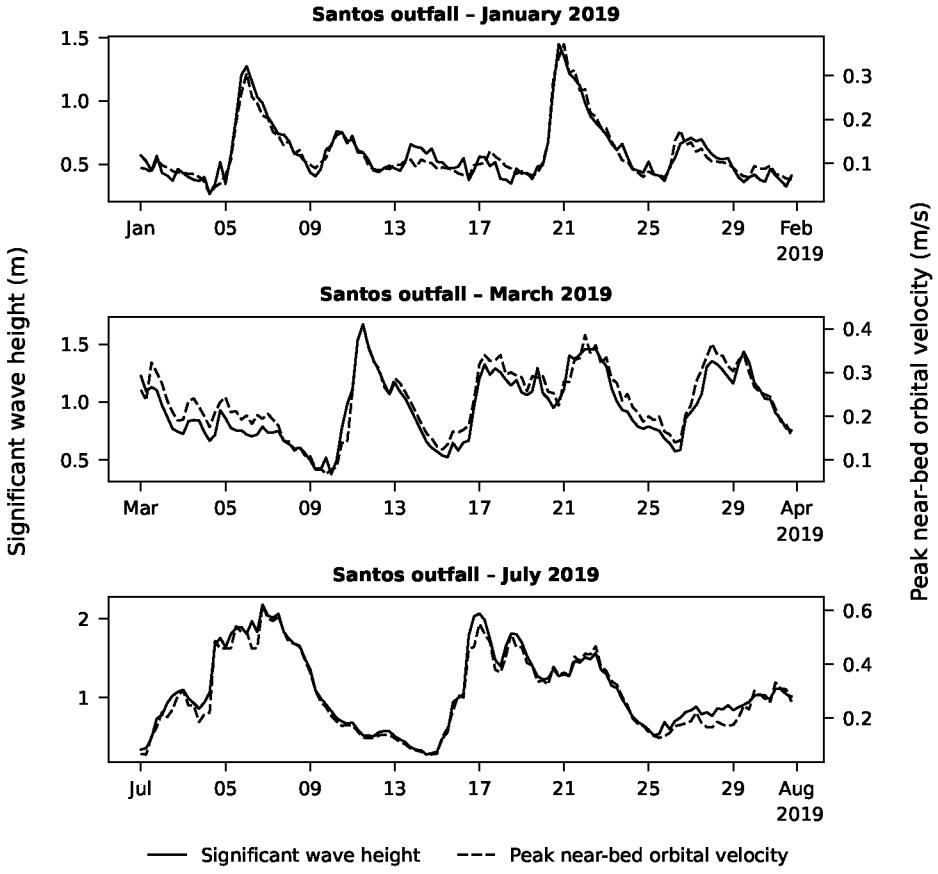

Figure 20: Significant wave height and peak near-bottom orbital velocity in the vicinity of the Santos outfall diffuser.

as a source or sink of bacteria concentration for the water column (e.g., Gao et al. 2013). This must be paired with sediment tracer studies (e.g., Pearson et al. 2021) to calibrate and validate the outfall sediment transport model.

The effects of strong extreme waves generated by meteorological events such as cold fronts and storms must be investigated because they have a high potential for sediment resuspension. Storm systems can produce waves with very long periods that can easily resuspend sediments at water depths that are normally under a deep-water wave regime. In fact, storm-induced waves can stir up fine sediments at depths of up to 40 m (Roberts et al. 2010). Furthermore, efforts could be done in integrating models of near-field sediment deposition from marine outfall jets (e.g., Neves and Fernando 1995; Bleninger and Carmer 2000; Lane-Serff and Moran 2005; Cuthbertson et al. 2008; Terfous et al. 2016) to coupled near-far-field modelling systems (e.g., Bleninger 2006; Morelissen et al. 2013; Horita et al. 2019). This would allow for a very detailed simulation of the non-linear interaction between currents, waves, sediment and outfall jets.

4 Conclusions

A coupled wave-current model with sediment transport was implemented in order to study the effects of waves on the transport and fate of sediments from submarine outfalls in relatively shallow waters. As a case study, an ensemble of five submarine outfalls in the coastal area of Baixada Santista, São Paulo state, Brazil, was selected. The model was implemented using operational data for 2019 provided by Sabesp. Comparison of results from a standalone hydrodynamic model (without waves) and the coupled wave-current model of Baixada Santista shows that waves have significant effects on the transport and fate of outfall solid particles.

If waves are not considered, the model simulates a continuous deposition process that, in the long term, results in unrealistic sediment deposits (about 20 cm/year). It was found that events of wave-induced sediment resuspension can occur in the vicinity of the outfall diffusers, even during the austral summer (January 2019), when waves are less energetic. In other seasons, waves are generally strong enough to hinder deposition and to remobilize sediment most of the time; for example, in months of average wave action and during the winter (March and July 2019, respectively). When considering wave-current interaction, month-end bed sediment deposits were up to 55% thinner under mild wave conditions and up to 90% thinner under strong waves.

The action of waves causes sediment to be dispersed over larger extents. If waves are not included in the model, outfall sediments tend to settle within 1–2 km from the diffusers. However, with wave-induced resuspension, the re-entrained sediment is transported further, reaching beaches and channels and eventually settling there. Furthermore, under mean and strong wave conditions, it was found that resuspended sediment can be transported westward over greater distances by wave-induced longshore currents. This affects the overall temporal distribution of sediment concentration in the water column in a way that relatively higher concentrations are more persistent over time.

The observed events of sediment resuspension respond to an increase in bed shear stresses due to wave-current interaction. At the depth of the diffusers, wave radiation stresses are not able to significantly intensify currents, but on average waves are large enough to produce elevated near-bed orbital velocities. The elliptical orbital motion of waves in the area can stir up bed sediments and re-entrain them in the water column as a result from a non-linear interaction between current and wave bed boundary layers. These findings were found to be consistent with linear wave theory.

The present study was not aimed to accurately quantify outfall sediment deposition nor to assess the

environmental impacts of these sediments. However, results provide phenomenological insights that may serve as a baseline for future studies on the matter. In order to evaluate potential impacts, it is necessary to perform detailed simulations of the sediment transport in the beaches and channels and accurately estimate sediment deposition. In addition, pollutants attached to sediment particles must be identified to implement water/sediment quality modeling. Numerical modeling must be paired with field studies on sediment tracing and bioaccumulation potential in order to validate the models and assess actual environmental concerns.

It is suggested that future studies consider the potential effects of surface waves on the design and operational conditions of submarine sewage outfalls. In particular, for outfalls that discharge in relatively shallow waters, the local wave climate must be analyzed to assess the potential for sediment resuspension. The results of coupled wave-current far-field models of outfall effluents can allow for understanding the fate of sediment-attached contaminants and identifying areas of potential environmental concern.

References

Abessa, D. M. S., R. S. Carr, B. R. F. Rachid, E. C. P. M. Sousa, M. A. Hortelani, and J. E. Sarkis. 2005. "Influence of a Brazilian sewage outfall on the toxicity and contamination of adjacent sediments." *Marine Pollution Bulletin* 50 (8): 875–885. ISSN: 0025-326X. https://doi.org/10.1016/j.marpolbul.2005.02.034.

Abessa, D. M. S., R. S. Carr, E. C. P. M. Sousa, B. R. F. Rachid, L. P. Zaroni, M. R. Gasparro, Y. A. Pinto, et al. 2008. "Integrative ecotoxicological assessment of contaminated sediments in a complex tropical estuarine system." In *Integrative ecotoxicological assessment of contaminated sediments in a complex tropical estuarine system,* edited by T. N. Hofer. New York: Nova Science Publishers, Inc.

Akdemir, T., and G. Dalgic. 2021. "The impact of the marine sewage outfalls on the sediment quality: The Black Sea and the Marmara case." *Saudi Journal of Biological Sciences* 28 (1): 238–246. ISSN: 1319-562X. https://doi.org/10.1016/j.sjbs.2020.09.055.

Allard, R., W. E. Rogers, S. N. Carroll, and K. V. Rushing. 2004. *Validation Test Report for the Simulating Waves Nearshore Model (SWAN): Cycle III, Version 40.11.* Technical report. Naval Research Laboratory, September 2, 2004.

Alosairi, Y., T. Pokavanich, and N. Alsulaiman. 2018. "Three-dimensional hydrodynamic modelling study of reverse estuarine circulation: Kuwait Bay." *Marine Pollution Bulletin* 127:82–96. ISSN: 0025-326X. https://doi.org/https://doi.org/10.1016/j.marpolbul.2017.11.049.

Arifin, A. N., S. Yano, and A. T. Lando. 2020. "Assessing effects of temporal changes in River water temperature on stratification in the Ariake Sea." *IOP Conference Series: Earth and Environmental Science* 419, no. 1 (June): 012157. https://doi.org/10.1088/1755-1315/419/1/012157.

Avnimelech, Y., G. Ritvo, L. E. Meijer, and M. Kochba. 2001. "Water content, organic carbon and dry bulk density in flooded sediments." *Aquacultural Engineering* 25, no. 1 (August): 25–33. https://doi.org/10.1016/s0144-8609(01)00068-1.

Aydoğan, B., and B. Ayat. 2021. "Performance evaluation of SWAN ST6 physics forced by ERA5 wind fields for wave prediction in an enclosed basin." *Ocean Engineering* 240:109936. ISSN: 0029-8018. https://doi.org/https://doi.org/10.1016/j.oceaneng.2021.109936.

Baptistelli, S. C. 2015. "Hydrodynamic Modeling: Application of Delft3D-FLOW in Santos Bay, São Paulo State, Brazil." In *Recent Progress in Desalination, Environmental and Marine Outfall Systems,* edited by M. Baawain, B. S. Choudri, M. Ahmed, and A. Purnama, 307–332. Cham, Switzerland: Springer International Publishing. ISBN: 978-3-319-19123-2. https://doi.org/10.1007/978-3-319-19123-2_22.

Battjes, J. A. 1974. "Computation of set-up, longshore currents, run-up and overtopping due to wind-generated waves." PhD diss., Delft University of Technology, June 5, 1974.

Beji, S., and J. A. Battjes. 1993. "Experimental investigation of wave propagation over a bar." *Coastal Engineering* 19, nos. 1-2 (February): 151–162. https://doi.org/10.1016/0378-3839(93)90022-z.

Belém, A. L., G. A. O. Moser, M. F. Palanch-Hans, F. F. Mauad, and L. L. Albertin. 2007. "Circulação/Estratificação Transiente no Complexo Estuarino de Santos: Comparações Entre o Estuário Interno e Área Costeira Adjacente Durante Sizigia." In *Anais do XVII Simpósio Brasileiro de Recursos Hídricos.* São Paulo, Brazil: Associação Brasileira de Recursos Hídricos (ABRHidro). https://www.abrhidro.org.br/SGCv3/publicacao.php?PUB=3&ID=19&SUMARIO=708.

Berbel, G. B. B., M. A. Hortellani, J. E. de Souza Sarkis, V. G. Chiozzini, D. I. T. Fávaro, B. O. Sutti, N. C. Sakazaki, and E. de Santis Braga. 2021. "Emerging contaminants (Rh, Pd, and Pt) in surface sediments from a Brazilian subtropical estuary influenced by anthropogenic activities." *Marine Pollution Bulletin* 163 (February): 111929. https://doi.org/10.1016/j.marpolbul.2020.111929.

Berzin, G. 1992. "Monitoring of the Santos Submarine Outfall, São Paulo, Brazil, 10 Years in Operation." *Water Science and Technology* 25, no. 9 (May): 59–71. https://doi.org/10.2166/wst.1992.0206.

Birocchi, P., M. Dottori, C. de Godoi Rezende Costa, and J. R. B. Leite. 2021. "Study of three domestic sewage submarine outfall plumes through the use of numerical modeling in the São Sebastião channel, São Paulo state, Brazil." *Regional Studies in Marine Science* 42:101647. ISSN: 2352-4855. https://doi.org/10.1016/j.rsma.2021.101647.

Bleck, R. 2002. "An oceanic general circulation model framed in hybrid isopycnic-Cartesian coordinates." *Ocean Modelling* 4 (1): 55–88. ISSN: 1463-5003. https://doi.org/10.1016/S1463-5003(01)00012-9.

Bleninger, T. 2006. "Coupled 3D hydrodynamic models for submarine outfalls: Environmental hydraulic design and control of multiport diffusers." PhD diss., University of Karlsruhe, June. https://doi.org/10.5445/KSP/1000006668.

Bleninger, T., and C. F. v. Carmer. 2000. "Sedimentation In Particle-Laden-Jets." Diploma thesis, University of Karlsruhe, April.

Bodeen, C. A., T. J. Hendricks, W. E. Frick, D. J. Baumgartner, J. E. Yerxa, and A. Steele. 1989. *User's Guide for SEDDEP: a Program for Computing Seabed Deposition Rates of Outfall Particulates in Coastal Marine Environments.* https://nepis.epa.gov/Exe/ZyPURL.cgi?Dockey=910096B9.txt.

Booij, N., R. C. Ris, and L. H. Holthuijsen. 1999. "A third-generation wave model for coastal regions: 1. Model description and validation." *Journal of Geophysical Research: Oceans* 104 (C4): 7649–7666. https://doi.org/https://doi.org/10.1029/98JC02622.

Bose, N. d. A., M. S. Ramos, G. S. Correia, C. W. Saidelles, L. Farina, C. K. Parise, and J. L. Nicolodi. 2022. "Assessing wind datasets and boundary conditions for wave hindcasting in the southern Brazil nearshore." *Computers & Geosciences* 159 (February): 104972. https://doi.org/10.1016/j.cageo.2021.104972.

Bouws, E., and G. J. Komen. 1983. "On the Balance Between Growth and Dissipation in an Extreme Depth-Limited Wind-Sea in the Southern North Sea." *Journal of Physical Oceanography* 13, no. 9 (September): 1653–1658. https://doi.org/10.1175/1520-0485(1983)013<1653:otbbga>2.0.co;2.

Boyd, C. E. 1995. *Bottom Soils, Sediment, and Pond Aquaculture.* New York: Chapman & Hall.

Bremer, T. S. v. d., and Ø. Breivik. 2017. "Stokes drift." *Philosophical Transactions of the Royal Society A: Mathematical, Physical and Engineering Sciences* 376, no. 2111 (December): 20170104. https://doi.org/10.1098/rsta.2017.0104.

Bühler, O. 2014. *Waves and Mean Flows.* Cambridge University Press, March. https://doi.org/10.1017/cbo9781107478701.

Carvalho, J. L. B., P. J. W. Roberts, and J. Roldão. 2002. "Field Observations of Ipanema Beach Outfall." *Journal of Hydraulic Engineering* 128, no. 2 (February): 151–160. https://doi.org/10.1061/(asce)0733-9429(2002)128:2(151).

Cesar, A., C. D. S. Pereira, A. R. Santos, D. M. de Sousa Abessa, N. Fernández, R. B. Choueri, and T. A. DelValls. 2006. "Ecotoxicological assessment of sediments from the Santos and São Vicente estuarine system – Brazil." *Brazilian Journal of Oceanography* 54 (1).

CETESB. 2022. *Qualidade das águas costeiras no estado de São Paulo 2021.* Technical report. São Paulo, Brazil: Companhia de Tecnologia de Saneamento Ambiental (CETESB).

Consórcio Partner/TetraTech. 2017. *Estudo de concepção de alternativas tecnológicas de tratamento de esgotos e de resíduos sólidos nos sistemas de esgotos da área insular dos municípios de Santos e São Vicente. Contrato CSS 30.392/14. Relatório final. Volume II de II: modelagem de transporte de sedimento. Fevereiro/2017. Revisão 0,* February 10, 2017.

Cuthbertson, A. J. S., D. D. Apsley, P. A. Davies, G. Lipari, and P. K. Stansby. 2008. "Deposition from Particle-Laden, Plane, Turbulent, Buoyant Jets." *Journal of Hydraulic Engineering* 134 (8): 1110–1122. https://doi.org/10.1061/(ASCE)0733-9429(2008)134:8(1110).

Dean, R. G., and R. A. Dalrymple. 1991. *Water Wave Mechanics for Engineers and Scientists.* World Scientific, January. https://doi.org/10.1142/1232.

Deigaard, R., J. B. Jakobsen, and J. Fredsøe. 1999. "Net sediment transport under wave groups and bound long waves." *Journal of Geophysical Research: Oceans* 104, no. C6 (June): 13559–13575. https://doi.org/10.1029/1999jc900072.

Deltares. 2020a. *Delft3D-FLOW, User Manual.* Delft, Netherlands: Deltares.

———. 2020b. *Delft3D-WAVE, User Manual.* Delft, Netherlands: Deltares.

Dingemans, M. W., A. C. Radder, and H. J. D. Vriend. 1987. "Computation of the driving forces of wave-induced currents." *Coastal Engineering* 11, nos. 5-6 (December): 539–563. https://doi.org/10.1016/0378-3839(87)90026-3.

Egbert, G. D., and S. Y. Erofeeva. 2002. "Efficient Inverse Modeling of Barotropic Ocean Tides." *Journal of Atmospheric and Oceanic Technology* (Boston MA, USA) 19 (2): 183–204. https://doi.org/10.1175/1520-0426(2002)019<0183:EIMOBO>2.0.CO;2.

Elias, E. P. L., D. J. R. Walstra, J. A. Roelvink, M. J. F. Stive, and M. D. Klein. 2001. "Hydrodynamic Validation of Delft3D with Field Measurements at Egmond." In *Coastal Engineering 2000: conference proceedings,* edited by B. L. Edge, 2714–2727. Sydney, Australia: American Society of Civil Engineers, July. https://doi.org/10.1061/40549(276)212.

Falkenberg, A. V., R. C. Barletta, L. Franklin, P. Ribeiro, P. G. D. Lara, T. Bleninger, A. B. Trevisan, and V. D. Santos. 2016. "Optimizing Outfall System Configurations Using Decision Support and Numerical Models. Case Study of Santa Catarina Island, Brazil." In *Proceedings of the International Symposium on Outfall Systems, 2016.* Ottawa, Canada: IAHR-IWA Joint Committee on Marine Outfall Systems, IAHR, May. https://www.iahr.org/library/infor?pid=9171.

Ferré, B., C. R. Sherwood, and P. L. Wiberg. 2010. "Sediment transport on the Palos Verdes shelf, California." *Continental Shelf Research* 30 (7): 761–780. ISSN: 0278-4343. https://doi.org/10.1016/j.csr.2010.01.011.

Fredsøe, J. 1984. "Turbulent Boundary Layer in Wave-current Motion." *Journal of Hydraulic Engineering* 110, no. 8 (August): 1103–1120. https://doi.org/10.1061/(asce)0733-9429(1984)110:8(1103).

Fukumoto, M. M., M. M. Mahiques, and M. G. Tessler. 2006. "Bottom faciology and sediment transport inSantos Bay, Southeastern Brazil." In *Journal of Coastal Research, SI 39 (Proccendigs of the 8th International CoastalSymposium),* 1737–1740. Itajaí, SC, Brazil.

Gao, G., R. A. Falconer, and B. Lin. 2013. "Modelling importance of sediment effects on fate and transport of enterococci in the Severn Estuary, UK." *Marine Pollution Bulletin* 67 (1): 45–54. ISSN: 0025-326X. https://doi.org/10.1016/j.marpolbul.2012.12.002.

Gelaro, R., W. McCarty, M. J. Suárez, R. Todling, A. Molod, L. Takacs, C. A. Randles, et al. 2017. "The Modern-Era Retrospective Analysis for Research and Applications, Version 2 (MERRA-2)." *Journal of Climate* (Boston MA, USA) 30 (14): 5419–5454. https://doi.org/10.1175/JCLI-D-16-0758.1.

Gerritsen, H., E. D. de Goede, F. W. Platzek, J. A. T. M. van Kester, M. Genseberger, and R. E. Uittenbogaard. 2008. *Validation Document Delft3D-FLOW, a software system for 3D flow simulations.* Technical report. Delft, Netherlands: Deltares.

Gkaragkouni, A., S. Sergiou, M. Geraga, H. Papaefthymiou, D. Christodoulou, and G. Papatheodorou. 2021. "Heavy Metal Distribution, Sources and Contamination Assessment in Polluted Marine Sediments: Keratsini Outfall Sewer Area, Saronikos Gulf, Greece." *Water, Air, & Soil Pollution* 232 (11): 477. ISSN: 0049-6979. https://doi.org/10.1007/s11270-021-05400-z.

Harari, J., C. França, and R. Camargo. 2008. "Climatology and hydrography of Santos Estuary." In *Perspectives on Integrated Coastal Zone Management in South America,* edited by R. Neves, J. Baretta, and M. Mateus, 147–160. IST Press.

Hasselmann, K., T. P. Barnett, E. Bouws, H. Carlson, D. E. Cartwright, K. Enke, J. A. Ewing, et al. 1973. *Measurements of wind-wave growth and swell decay during the Joint North Sea Wave Project (JONSWAP).* Research report. Hamburg, Germany: Deutsche Hydrographisches Institut.

Herring, J. R. 1980. "Wastewater Particle Dispersion in the Southern California Offshore Region." Chap. 13 in *Particulates in Water,* edited by M. C. Kavanaugh and J. O. Leckie, 189:283–304. Advances in Chemistry. Washington, D.C.: American Chemical Society. https://doi.org/10.1021/ba-1980-0189.ch013.

Hersbach, H., B. Bell, P. Berrisford, S. Hirahara, A. Horányi, J. Muñoz-Sabater, J. Nicolas, et al. 2020. "The ERA5 global reanalysis." *Quarterly Journal of the Royal Meteorological Society* 146 (730): 1999–2049. https://doi.org/10.1002/qj.3803.

Hershelman, G. P., H. A. Schafer, T.-K. Jan, and D. R. Young. 1981. "Metals in marine sediments near a large California municipal outfall." *Marine Pollution Bulletin* 12 (4): 131–134. ISSN: 0025-326X. https://doi.org/10.1016/0025-326X(81)90442-2.

Ho, M., J. M. Molemaker, F. Kessouri, J. C. McWilliams, and T. W. Gallien. 2021. "High-Resolution Nonhydrostatic Outfall Plume Modeling: Cross-Flow Validation." *Journal of Hydraulic Engineering* 147 (8): 04021028. https://doi.org/10.1061/(ASCE)HY.1943-7900.0001896.

Hodgins, D. O., S. L. M. Hodgins, and R. E. Corbett. 2000. "Modeling sewage solids deposition patterns for the Five Fingers Island outfall, Nanaimo, British Columbia." In *Proceedings of the Watershed Management 2000 Conference,* 2000:991–1008. Water Environment Federation, January. https://doi.org/10.2175/193864700785149008. https://www.accesswater.org/?id=-287626.

Horita, C. O., T. B. Bleninger, R. Morelissen, and J. L. B. de Carvalho. 2019. "Dynamic coupling of a near with a far field model for outfall discharges." *Journal of Applied Water Engineering and Research* 7, no. 4 (October): 295–313. https://doi.org/10.1080/23249676.2019.1685413.

Huff, T. P., R. A. Feagin, and J. Figlus. 2022. "Delft3D as a Tool for Living Shoreline Design Selection by Coastal Managers." *Frontiers in Built Environment* 8. ISSN: 2297-3362. https://doi.org/10.3389/fbuil.2022.926662.

Inan, A. 2019. "Modeling of Hydrodynamics and Dilution in Coastal Waters." *Water* 11 (1). ISSN: 2073-4441. https://doi.org/10.3390/w11010083.

Innocentini, V., E. Caetano, and J. T. Carvalho. 2014. "A Procedure for Operational Use of Wave Hindcasts to Identify Landfall of Heavy Swell." *Weather and Forecasting* 29, no. 2 (April): 349–365. https://doi.org/10.1175/waf-d-13-00077.1.

Iouzzi, N., L. Mouakkir, M. Ben Meftah, M. Chagdali, and D. Loudyi. 2022. "SWAN Modeling of Dredging Effect on the Oued Sebou Estuary." *Water* 14 (17). ISSN: 2073-4441. https://doi.org/10.3390/w14172633.

Kaiser, J., I. C. M. Nogueira, R. M. Campos, C. E. Parente, R. P. Martins, and W. C. Belo. 2022. "Evaluation of wave model performance in the South Atlantic Ocean: a study about physical parameterization and wind forcing calibration." *Ocean Dynamics* 72, no. 2 (January): 137–150. https://doi.org/10.1007/s10236-021-01495-4.

Kalnejais, L. H., W. R. Martin, and M. H. Bothner. 2010. "The release of dissolved nutrients and metals from coastal sediments due to resuspension." *Marine Chemistry* 121 (1): 224–235. ISSN: 0304-4203. https://doi.org/10.1016/j.marchem.2010.05.002.

Kanamitsu, M., W. Ebisuzaki, J. Woollen, S.-K. Yang, J. J. Hnilo, M. Fiorino, and G. L. Potter. 2002. "NCEP–DOE AMIP-II Reanalysis (R-2)." *Bulletin of the American Meteorological Society* (Boston MA, USA) 83 (11): 1631–1644. https://doi.org/10.1175/BAMS-83-11-1631.

Kim, M., M. Ligaray, Y. S. Kwon, S. Kim, S. Baek, J. Pyo, G. Baek, et al. 2021. "Designing a marine outfall to reduce microbial risk on a recreational beach: Field experiment and modeling." *Journal of Hazardous Materials* 409:124587. ISSN: 0304-3894. https://doi.org/10.1016/j.jhazmat.2020.124587.

Komen, G. J., L. Cavaleri, M. Donelan, K. Hasselmann, S. Hasselmann, and P. A. E. M. Janssen. 1994. *Dynamics and Modelling of Ocean Waves.* Cambridge: Cambridge University Press. https://doi.org/10.1017/CBO9780511628955.

Kuik, A. J., G. v. Vledder, and L. H. Holthuijsen. 1988. "A Method for the Routine Analysis of Pitch-and-Roll Buoy Wave Data." *Journal of Physical Oceanography* 18, no. 7 (July): 1020–1034. https://doi.org/10.1175/1520-0485(1988)018<1020:amftra>2.0.co;2.

Lane-Serff, G. F., and T. J. Moran. 2005. "Sedimentation from Buoyant Jets." *Journal of Hydraulic Engineering* 131 (3): 166–174. https://doi.org/10.1061/(ASCE)0733-9429(2005)131:3(166).

Lee, H. J., M. A. Noble, and J. Xu. 2003. "Sediment Transport and Deposition Processes Near Ocean Outfalls in Southern California." In *Contaminated Sediments: Characterization, Evaluation, Mitigation/Restoration, and Management Strategy Performance, ASTM STP 1442,* edited by J. Locat, R. Galvez-Cloutier, R. C. Chaney, and K. R. Demars, 253–265. West Conshohocken, PA: ASTM International. ISBN: 978-0-8031-3466-9. https://doi.org/10.1520/STP11567S.

Lenstra, K. J. H., S. R. P. M. Pluis, W. Ridderinkhof, G. Ruessink, and M. van der Vegt. 2019. "Cyclic channel-shoal dynamics at the Ameland inlet: the impact on waves, tides, and sediment transport." *Ocean Dynamics* 69, no. 4 (April): 409–425. ISSN: 1616-7228. https://doi.org/10.1007/s10236-019-01249-3.

Longuet-Higgins, M. S. 1953. "Mass transport in water waves." *Philosophical Transactions of the Royal Society of London. Series A, Mathematical and Physical Sciences* 245, no. 903 (March): 535–581. https://doi.org/10.1098/rsta.1953.0006.

———. 1972. "Recent Progress in the Study of Longshore Currents." In *Waves on Beaches and Resulting Sediment Transport,* edited by R. E. Meyer, 203–248. Academic Press. https://doi.org/10.1016/b978-0-12-493250-0.50011-4.

Longuet-Higgins, M. S., and R. W. Stewart. 1960. "Changes in the form of short gravity waves on long waves and tidal currents." *Journal of Fluid Mechanics* 8, no. 04 (September): 565. https://doi.org/10.1017/s0022112060000803.

Magris, R., M. Marta-Almeida, J. Monteiro, and N. Ban. 2019. "A modelling approach to assess the impact of land mining on marine biodiversity: Assessment in coastal catchments experiencing catastrophic events (SW Brazil)." *Science of The Total Environment* 659 (April): 828–840. https://doi.org/10.1016/j.scitotenv.2018.12.238.

Maruya, K. A., D. E. Vidal-Dorsch, S. M. Bay, J. W. Kwon, K. Xia, and K. L. Armbrust. 2012. "Organic contaminants of emerging concern in sediments and flatfish collected near outfalls discharging treated wastewater effluent to the Southern California Bight." *Environmental Toxicology and Chemistry* 31 (12): 2683–2688. https://doi.org/10.1002/etc.2003.

Megahan, W. F. 1999. "Sediment pollution." In *Environmental Geology,* 552–553. Dordrecht, Netherlands: Springer Netherlands. ISBN: 978-1-4020-4494-6. https://doi.org/10.1007/1-4020-4494-1_297.

Mendes, J., R. Ruela, A. Picado, J. P. Pinheiro, A. S. Ribeiro, H. Pereira, and J. M. Dias. 2021. "Modeling Dynamic Processes of Mondego Estuary and Óbidos Lagoon Using Delft3D." *Journal of Marine Science and Engineering* 9 (1). ISSN: 2077-1312. https://doi.org/10.3390/jmse9010091.

Moon, H.-B., S.-P. Yoon, R.-H. Jung, and M. Choi. 2008. "Wastewater treatment plants (WWTPs) as a source of sediment contamination by toxic organic pollutants and fecal sterols in a semi-enclosed bay in Korea." *Chemosphere* 73 (6): 880–889. ISSN: 0045-6535. https://doi.org/10.1016/j.chemosphere.2008.07.038.

Morelissen, R., T. van der Kaaij, and T. Bleninger. 2013. "Dynamic coupling of near field and far field models for simulating effluent discharges." *Water Science and Technology* 67, no. 10 (May): 2210–2220. ISSN: 0273-1223. https://doi.org/10.2166/wst.2013.081.

Mrša Haber, I., T. Legović, L. Kranjčević, and M. Cukrov. 2020. "Simulation of pollutants spreading from a sewage outfall in the Rijeka Bay." *Mediterranean Marine Science* 21, no. 1 (May): 116–128. https://doi.org/10.12681/mms.20467.

Murakami, M., Y. Oonishi, and H. Kunishi. 1985. "A numerical simulation of the distribution of water temperature and salinity in the Seto Inland Sea." *Journal of the Oceanographical Society of Japan* 41 (4): 213–224. ISSN: 0029-8131. https://doi.org/10.1007/BF02109271.

Neill, S. P., and M. R. Hashemi. 2018. "Ocean Modelling for Resource Characterization." In *Fundamentals of Ocean Renewable Energy,* 193–235. Elsevier. https://doi.org/10.1016/b978-0-12-810448-4.00008-2.

Neves, M. J., and H. J. S. Fernando. 1995. "Sedimentation of particles from jets discharged by ocean outfalls: a theoretical and laboratory study." *Water Science and Technology* 32, no. 2 (July): 133–139. ISSN: 0273-1223. https://doi.org/10.2166/wst.1995.0088.

Neves, R. 2006. "Modelling Applied to Waste Disposal Systems. Application of Mohid for Simulating Trophic Activity in The Tagus and for Assessing the Impact of Costa do Estoril Submarine Outfall." In *Submarine outfalls: design, compliance and environmental monitoring,* edited by C. C. Lamparelli and J. P. Ortiz, 147–169. São Paulo, Brazil: Secretaria do Meio Ambiente do Estado de São Paulo. ISBN: 85-86624-49-7.

Nielsen, P. 1992. *Coastal Bottom Boundary Layers and Sediment Transport.* WORLD SCIENTIFIC, July. https://doi.org/10.1142/1269.

Nusbaum, I., and R. M. Garver. 1955. "Survival of Coliform Organisms in Pacific Ocean Coastal Waters." *Sewage and Industrial Wastes* 27 (12): 1383–1390. Accessed October 26, 2022. http://www.jstor.org/stable/25032950.

Ormondt, M. v., K. Nederhoff, and A. v. Dongeren. 2020. "Delft Dashboard: a quick set-up tool for hydrodynamic models." *Journal of Hydroinformatics* 22, no. 3 (February): 510–527. ISSN: 1464-7141. https://doi.org/10.2166/hydro.2020.092.

Ostoich, M., M. Ghezzo, G. Umgiesser, M. Zambon, L. Tomiato, F. Ingegneri, and G. Mezzadri. 2018. "Modelling as decision support for the localisation of submarine urban wastewater outfall: Venice lagoon (Italy) as a case study." *Environmental Science and Pollution Research* 25 (34): 34306–34318. ISSN: 0944-1344. https://doi.org/10.1007/s11356-018-3316-0.

Pearson, S. G., B. C. van Prooijen, J. Poleykett, M. Wright, K. Black, and Z. B. Wang. 2021. "Tracking fluorescent and ferrimagnetic sediment tracers on an energetic ebb-tidal delta to monitor grain size-selective dispersal." *Ocean & Coastal Management* 212 (October): 105835. https://doi.org/10.1016/j.ocecoaman.2021.105835.

Pianca, C., P. L. F. Mazzini, and E. Siegle. 2010. "Brazilian offshore wave climate based on NWW3 reanalysis." *Brazilian Journal of Oceanography* 58, no. 1 (March): 53–70. https://doi.org/10.1590/s1679-87592010000100006.

Pokavanich, T., K. Nadaoka, and A. C. Blanco. 2008. "Comprehensive Circulation and Water Quality Investigation of the Coastal Lagoon: Puerto Galera, the Philippines." In *Proceedings of the 8th International Conference on Hydro-Science and Engineering,* edited by S. S. Y. Wang. Nagoya, Japan: Nagoya Hydraulic Research Institute for River Basin Management, September. https://hdl.handle.net/20.500.11970/110193.

Pritchard, D., G. Savidge, and B. Elsäßer. 2013. "Coupled hydrodynamic and wastewater plume models of Belfast Lough, Northern Ireland: A predictive tool for future ecological studies." *Marine Pollution Bulletin* 77 (1): 290–299. ISSN: 0025-326X. https://doi.org/10.1016/j.marpolbul.2013.09.046.

Reed, S., M. Clark, R. Thompson, and K. A. Hughes. 2018. "Microplastics in marine sediments near Rothera Research Station, Antarctica." *Marine Pollution Bulletin* 133:460–463. ISSN: 0025-326X. https://doi.org/10.1016/j.marpolbul.2018.05.068.

Ris, R. C., L. H. Holthuijsen, and N. Booij. 1999. "A third-generation wave model for coastal regions: 2. Verification." *Journal of Geophysical Research: Oceans* 104, no. C4 (April): 7667–7681. https://doi.org/10.1029/1998jc900123.

Rittenberg, S. C., T. Mittwer, and D. Iyler. 1958. "Coliform Bacteria in Sediments Around Three Marine Sewage Outfalls1." *Limnology and Oceanography* 3 (1): 101–108. https://doi.org/10.4319/lo.1958.3.1.0101.

Roberts, P. J. W. 1991. "Ocean outfalls." *Critical Reviews in Environmental Control* 20 (5-6): 311–339. https://doi.org/10.1080/10643389109388404.

Roberts, P. J. W., H. J. Salas, F. M. Reiff, M. Libhaber, A. Labbe, and J. C. Thomson. 2010. *Marine Wastewater Outfalls and Treatment Systems.* IWA Publishing, August. ISBN: 9781780401669. https://doi.org/10.2166/9781780401669. eprint: https://iwaponline.com/book-pdf/142287/wio9781780401669.pdf.

Roberts, P. J. W., and B. Villegas. 2017. "Modeling and Design of the Buenos Aires Outfalls." *Journal of Hydraulic Engineering* 143 (2): 05016007. https://doi.org/10.1061/(ASCE)HY.1943-7900.0001244.

Rusu, L. 2022. "The near future expected wave power in the coastal environment of the Iberian Peninsula." *Renewable Energy* 195:657–669. ISSN: 0960-1481. https://doi.org/https://doi.org/10.1016/j.renene.2022.06.047.

Saha, S., S. Moorthi, X. Wu, J. Wang, S. Nadiga, P. Tripp, D. Behringer, et al. 2014. "The NCEP Climate Forecast System Version 2." *Journal of Climate* (Boston MA, USA) 27 (6): 2185–2208. https://doi.org/10.1175/JCLI-D-12-00823.1.

Santos, D. M. dos, L. Buruaem, R. M. Gonçalves, M. Williams, D. M. S. Abessa, R. Kookana, and M. R. R. de Marchi. 2018. "Multiresidue determination and predicted risk assessment of contaminants of emerging concern in marine sediments from the vicinities of submarine sewage outfalls." *Marine Pollution Bulletin* 129, no. 1 (April): 299–307. https://doi.org/10.1016/j.marpolbul.2018.02.048.

Schettini, C. A. F., E. C. Truccolo, J. A. D. Mattos, and D. C. D. A. Benevides. 2019. "Tides and sea level variability decomposition in the Port of Santos Waterway." *Brazilian Journal of Oceanography* 67 (October). ISSN: 1982-436X. https://doi.org/10.1590/s1679-87592019026506707.

Smith, G. A., M. Hemer, D. Greenslade, C. Trenham, S. Zieger, and T. Durrant. 2021. "Global wave hindcast with Australian and Pacific Island Focus: From past to present." *Geoscience Data Journal* 8 (1): 24–33. https://doi.org/10.1002/gdj3.104.

Soto-Jiménez, M., F. Páez-Osuna, and F. Morales-Hernández. 2001. "Selected trace metals in oysters (Crassostrea iridescens) and sediments from the discharge zone of the submarine sewage outfall in Mazatlán Bay (southeast Gulf of California): chemical fractions and bioaccumulation factors." *Environmental Pollution* 114 (3): 357–370. ISSN: 0269-7491. https://doi.org/10.1016/S0269-7491(00)00239-6.

Soulsby, R. L., L. Hamm, G. Klopman, D. Myrhaug, R. R. Simons, and G. P. Thomas. 1993. "Wave-current interaction within and outside the bottom boundary layer." *Coastal Engineering* 21, nos. 1-3 (December): 41–69. https://doi.org/10.1016/0378-3839(93)90045-a.

Soulsby, R. L., and J. D. Humphery. 1990. "Field Observations of Wave-Current Interaction at the Sea Bed." In *Water Wave Kinematics,* edited by A. Tørum and O. T. Gudmestad, 178:413–428. NATO ASI Series. Dordrecht, Netherlands: Springer. https://doi.org/10.1007/978-94-009-0531-3_25.

Sousa, E. C. P. M., L. P. Zaroni, M. R. Gasparro, and C. D. S. Pereira. 2014. "Review Of Ecotoxicological Studies Of The Marine And Estuarine Environments Of The Baixada Santista (São Paulo, Brazil)." *Brazilian Journal of Oceanography* 62, no. 2 (July): 133–147. ISSN: 1679-8759. https://doi.org/10.1590/S1679-87592014063006202.

Stech, J. L., and J. A. Lorenzzetti. 1992. "The response of the South Brazil Bight to the passage of wintertime cold fronts." *Journal of Geophysical Research: Oceans* 97 (C6): 9507–9520. https://doi.org/10.1029/92JC00486.

Stein, L. P., and E. Siegle. 2019. "Santos beach morphodynamics under high-energy conditions." *Revista Brasileira de Geomorfologia* 20, no. 3 (July). https://doi.org/10.20502/rbg.v20i3.1419.

Stokes, G. G. 1847. "On the theory of oscillatory waves." *Transactions of the Cambridge Philosophical Society* 8 (March 1, 1847): 441–455.

Stopa, J. E. 2018. "Wind forcing calibration and wave hindcast comparison using multiple reanalysis and merged satellite wind datasets." *Ocean Modelling* 127 (July): 55–69. https://doi.org/10.1016/j.ocemod.2018.04.008.

Tate, P. M., C. J. Holden, and D. J. Tate. 2019. "Influence of plume advection and particle settling on wastewater dispersion and distribution." *Marine Pollution Bulletin* 145:678–690. ISSN: 0025-326X. https://doi.org/10.1016/j.marpolbul.2019.05.059.

Tate, P. M., S. Scaturro, and B. Cathers. 2016. "Marine Outfalls." In *Springer Handbook of Ocean Engineering,* edited by M. R. Dhanak and N. I. Xiros, 711–740. Cham, Switzerland: Springer International Publishing. ISBN: 978-3-319-16649-0. https://doi.org/10.1007/978-3-319-16649-0_32.

Terfous, A., S. Chiban, and A. Ghenaim. 2016. "Modeling sediment deposition from marine outfall jets." *Environmental Technology* 37 (15): 1865–1874. https://doi.org/10.1080/09593330.2015.1135988.

Tomicic, B., A. Lützen, and O. Mark. 2001. "Integrated Modelling of the Sewer System and the Receiving Waters for the Island of Ischia." In *Urban Drainage Modeling; proceedings of the specialty symposium held in conjunction with the World Water and Environmental Resources Congress,* edited by R. W. Brashear and C. Maksimovic, 548–557. Orlando, FL: ASCE Environmental and Water Resources Institute; IAHR-IWA Joint Committee on Urban Drainage, American Society of Civil Engineers, May. https://doi.org/10.1061/40583(275)52.

Tozer, B., D. T. Sandwell, W. H. F. Smith, C. Olson, J. R. Beale, and P. Wessel. 2019. "Global Bathymetry and Topography at 15 Arc Sec: SRTM15+." *Earth and Space Science* 6 (10): 1847–1864. https://doi.org/10.1029/2019EA000658.

Uchiyama, Y., E. Y. Idica, J. C. McWilliams, and K. D. Stolzenbach. 2014. "Wastewater effluent dispersal in Southern California Bays." *Continental Shelf Research* 76:36–52. ISSN: 0278-4343. https://doi.org/10.1016/j.csr.2014.01.002.

Vacchi, F. I., A. dos Santos, M. C. Artal, G. R. Magalhães, J. A. de Souza Vendemiatti, and G. de Aragão Umbuzeiro. 2019. "Parhyale hawaiensis as a promising alternative organism for monitoring acute toxicity of sediments under the influence of submarine outfalls." *Marine Pollution Bulletin* 149 (December): 110658. https://doi.org/10.1016/j.marpolbul.2019.110658.

Veríssimo, F., and F. Martins. 2016. "Impact of Albufeira Bay (Portugal) Outfall Plumes in Bathing Water Quality, a Modelling Approach." In *Proceedings of the International Symposium on Outfall Systems, 2016.* Ottawa, Canada: IAHR-IWA Joint Committee on Marine Outfall Systems, IAHR, May. http://www.iahr.org.cn/library/infor?pid=9188.

Violante-Carvalho, N., C. E. Parente, I. S. Robinson, and L. M. P. Nunes. 2001. "On the Growth of Wind-Generated Waves in a Swell-Dominated Region in the South Atlantic." *Journal of Offshore Mechanics and Arctic Engineering* 124, no. 1 (August): 14–21. https://doi.org/10.1115/1.1423636.

Vittori, G., and P. Blondeaux. 1996. "Mass transport under sea waves propagating over a rippled bed." *Journal of Fluid Mechanics* 314 (May): 247–265. https://doi.org/10.1017/s0022112096000304.

Vledder, G. v., M. Zijlema, and L. H. Holthuijsen. 2011. "Revisiting the JONSWAP Bottom Friction Formulation." In *Proceedings of 32nd International Conference on Coastal Engineering, Shanghai, China, 2010,* edited by J. M. Smith and P. Lynett. January 27, 2011. https://doi.org/https://doi.org/10.9753/icce.v32.waves.41.

Wasserman, J. C., A. A. P. Freitas-Pinto, and D. Amouroux. 2000. "Mercury Concentrations in Sediment Profiles of a Degraded Tropical Coastal Environment." *Environmental Technology* 21 (3): 297–305. https://doi.org/10.1080/09593332108618117.

Watkins, J. G. 1961. "Foraminiferal Ecology around the Orange County, California, Ocean Sewer Outfall." *Micropaleontology* 7 (2): 199–206. Accessed October 26, 2022. http://www.jstor.org/stable/1484279.

Whitham, G. B. 1999. *Linear and Nonlinear Waves.* John Wiley & Sons, Inc., June. https://doi.org/10.1002/9781118032954.

Wiberg, P. L., and C. R. Sherwood. 2008. "Calculating wave-generated bottom orbital velocities from surface-wave parameters." *Computers & Geosciences* 34, no. 10 (October): 1243–1262. https://doi.org/10.1016/j.cageo.2008.02.010.

Willmott, C. J., S. M. Robeson, and K. Matsuura. 2011. "A refined index of model performance." *International Journal of Climatology* 32, no. 13 (September): 2088–2094. https://doi.org/10.1002/joc.2419.

Wu, Y., L. Washburn, and B. H. Jones. 1991. "Mixing and dispersion processes in the vicinity of an ocean outfall system in Southern California." In *Coastal Zone '91: Proceedings of the Seventh Symposium on Coastal and Ocean Management,* edited by O. T. Magoon, H. Converse, V. Tippie, L. T. Tobin, and D. Clark. Long Beach, CA: American Society of Civil Engineers. https://cedb.asce.org/CEDBsearch/record.jsp?dockey=0071341.

Zhang, X., R. Simons, J. Zheng, and C. Zhang. 2022. "A review of the state of research on wave-current interaction in nearshore areas." *Ocean Engineering* 243 (January): 110202. https://doi.org/10.1016/j.oceaneng.2021.110202.

Zhao, L., Z. Chen, and K. Lee. 2011. "Modelling the dispersion of wastewater discharges from offshore outfalls: a review." *Environmental Reviews* 19 (NA): 107–120. https://doi.org/10.1139/a10-025.